



# **A Brief Summary of Different Tritium Sources for a Tritiumless Hybrid Reactor**

**G.A. Moses**

**October 1979**

**UWFDM-317**

***FUSION TECHNOLOGY INSTITUTE  
UNIVERSITY OF WISCONSIN  
MADISON WISCONSIN***

# **A Brief Summary of Different Tritium Sources for a Tritiumless Hybrid Reactor**

G.A. Moses

Fusion Technology Institute  
University of Wisconsin  
1500 Engineering Drive  
Madison, WI 53706

<http://fti.neep.wisc.edu>

October 1979

UWFDM-317

### "LEGAL NOTICE"

"This work was prepared by the University of Wisconsin as an account of work sponsored by the Electric Power Research Institute, Inc. ("EPRI"). Neither EPRI, members of EPRI, the University of Wisconsin, nor any person acting on behalf of either:

"a. Makes any warranty or representation, express or implied, with respect to the accuracy, completeness, or usefulness of the information contained in this report, or that the use of any information, apparatus, method, or process disclosed in this report may not infringe privately owned rights; or

"b. Assumes any liabilities with respect to the use of, or for damages resulting from the use of, any information, apparatus, method or process disclosed in this report."

A Brief Summary of Different Tritium  
Sources for a Tritiumless Hybrid Reactor

Gregory A. Moses

October 1979

Fusion Engineering Program  
Department of Nuclear Engineering  
University of Wisconsin  
Madison, Wisconsin 53706

UWFDM-317

## I. Introduction

The impact of fusion energy might be greatly amplified through the development of fusion-fission hybrid reactors, where the 14 MeV fusion neutrons are used to breed fissile fuel in addition to the tritium that is needed to fuel the fusion reactor. The fissile fuel produced in such hybrid reactors can be periodically removed, reprocessed and burnt in conventional light water reactors. Hence the ultimate energy released per fusion reaction can be amplified from ~20 MeV to 200-300 MeV when the subsequent fission reactions are included in the total. Furthermore, this energy multiplication greatly relaxes the economic constraints that the fusion reactor must meet to be competitive with other energy sources and it relaxes the fusion performance that is necessary to meet these economic criteria. This latter point has the additional effect that the hybrid reactor could be introduced at an earlier time than the pure fusion reactor.

However, this early introduction of the hybrid depends upon the rapid development of the support systems for the reactor.

One such system of particular importance is the tritium breeding process in the blanket and the recovery of the bred tritium. This system has been studied extensively at the conceptual level in fusion reactor conceptual designs but has never been tested in a laboratory environment. This situation leads to the following questions:

- (1) Is it technically simpler to remove the tritium breeding function from the hybrid and produce the tritium externally, in dedicated tritium producing fission or fusion reactors or in modified power producing fission reactors?

(2) Is one of these options more economical than producing both fissile fuel and tritium in the hybrid?

(3) Will removing the tritium breeding function from the hybrid allow an earlier date of introduction?

The answers to these questions require an analysis of many different factors. The technical simplicity of the hybrid will depend upon the impact of removing the tritium breeding process. Recall that the hybrid reactor must still have systems to handle the unburnt tritium from the fusion plasma. Also the blanket radioactivity will not be reduced because of the fission products generated in the fission fuel. The economics will depend upon the total cost of electricity generated by the system of hybrid plus dedicated tritium source, etc. This in turn will depend upon the breeding performance of each reactor and its costs.

In this report we survey the possible sources of tritium other than the hybrid reactor itself. These sources include:

- The U.S. stockpile
- Production reactors<sup>(2)</sup>
- Light Water Reactors<sup>(1)</sup>
- Modified Light Water Reactors<sup>(1)</sup>
- Liquid Metal Fast Breeder Reactors<sup>(3)</sup>
- Heavy Water Reactors<sup>(1)</sup>
- Fuel Reprocessing Plants<sup>(1)</sup>
- Dedicated Fusion Reactors

Each of these sources is described in some detail and estimates of the tritium production capabilities of each are given. Finally, conclusions are given regarding the viability of each of these sources in the context of providing tritium to a hybrid reactor.

## II. The U.S. Stockpile

The United States' tritium stockpile is maintained for the nuclear weapons program. The magnitude of this stockpile is not known and we must presume that it is not available for commercial fusion purposes.

## III. Production Reactors

The tritium that is needed to support the nuclear weapons program is made in fission production reactors at the Savannah River Plant. Some tritium has also been made in the N-Reactor at the Hanford Site. Because these are proven tritium producing technologies we shall describe them in some detail.

### III.A. Savannah River Production Reactors

The Savannah River reactors are thermal reactors cooled and moderated with heavy water. They are descendants of the early NPD Reactor. As shown in Figs. 1 and 2, a reactor consists of a tank 17 ft. in diameter and 15 ft. high. The core of the reactor contains 612 fuel and/or target assemblies and 61 control assemblies, all arranged in a hexagonal pattern as shown in Figs. 3 and 4. The tritium-producing elements are placed around the reflector while the Pu ones are dispersed in the core. The  $D_2O$  exits the reactor tank through six symmetrically located nozzles, and then flows through six external loops. Each loop has one pump and two heat exchangers in parallel. Returning from the heat exchangers, most of the  $D_2O$  flows to the plenum via six nozzles located along its rim. The remainder of the  $D_2O$  flow goes to a header below the reactor tank and supplies cooling to the control assemblies. The  $D_2O$  flows at high velocity from the plenum down the fuel and target assemblies and enters the moderator space at the bottom of the tank. The  $D_2O$ , now acting as a moderator, flows upward, outward, and then downward in a three-dimensional path across the bank of assemblies to the exit nozzles. The reactor operates with single-phase flow throughout the

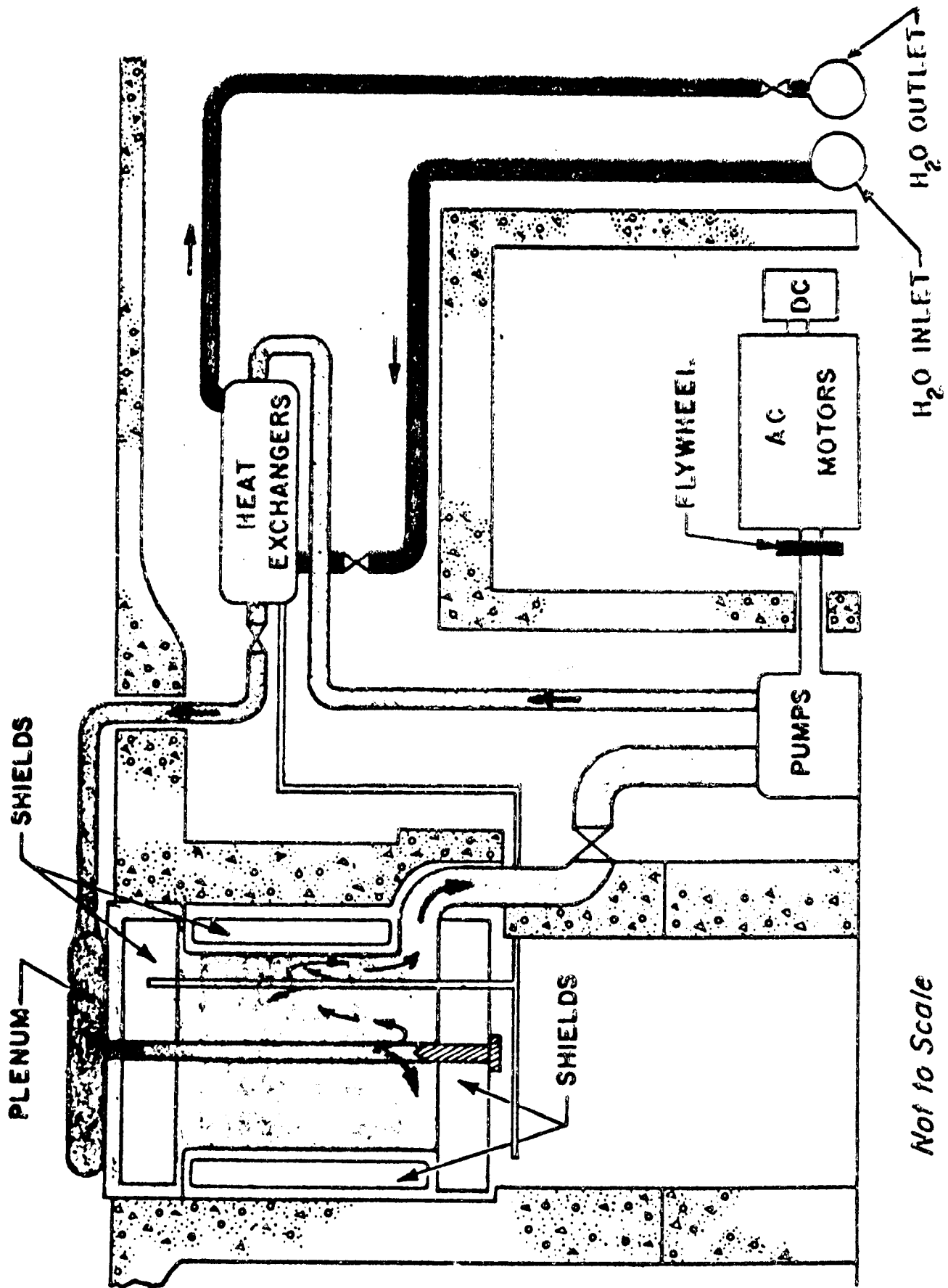


FIGURE 1 Schematic Diagram of Savannah River Reactor



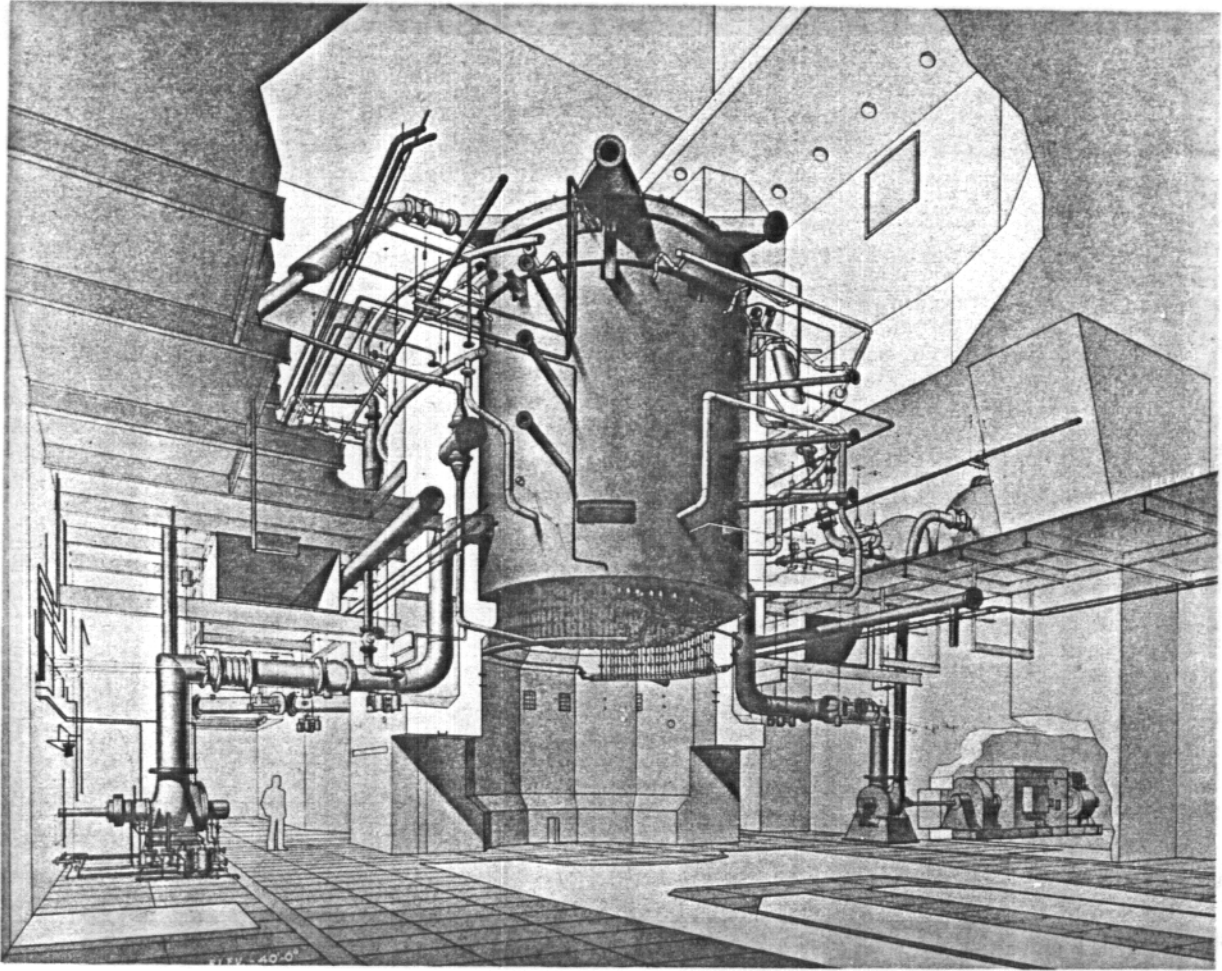


FIGURE 2

Savannah River Reactor

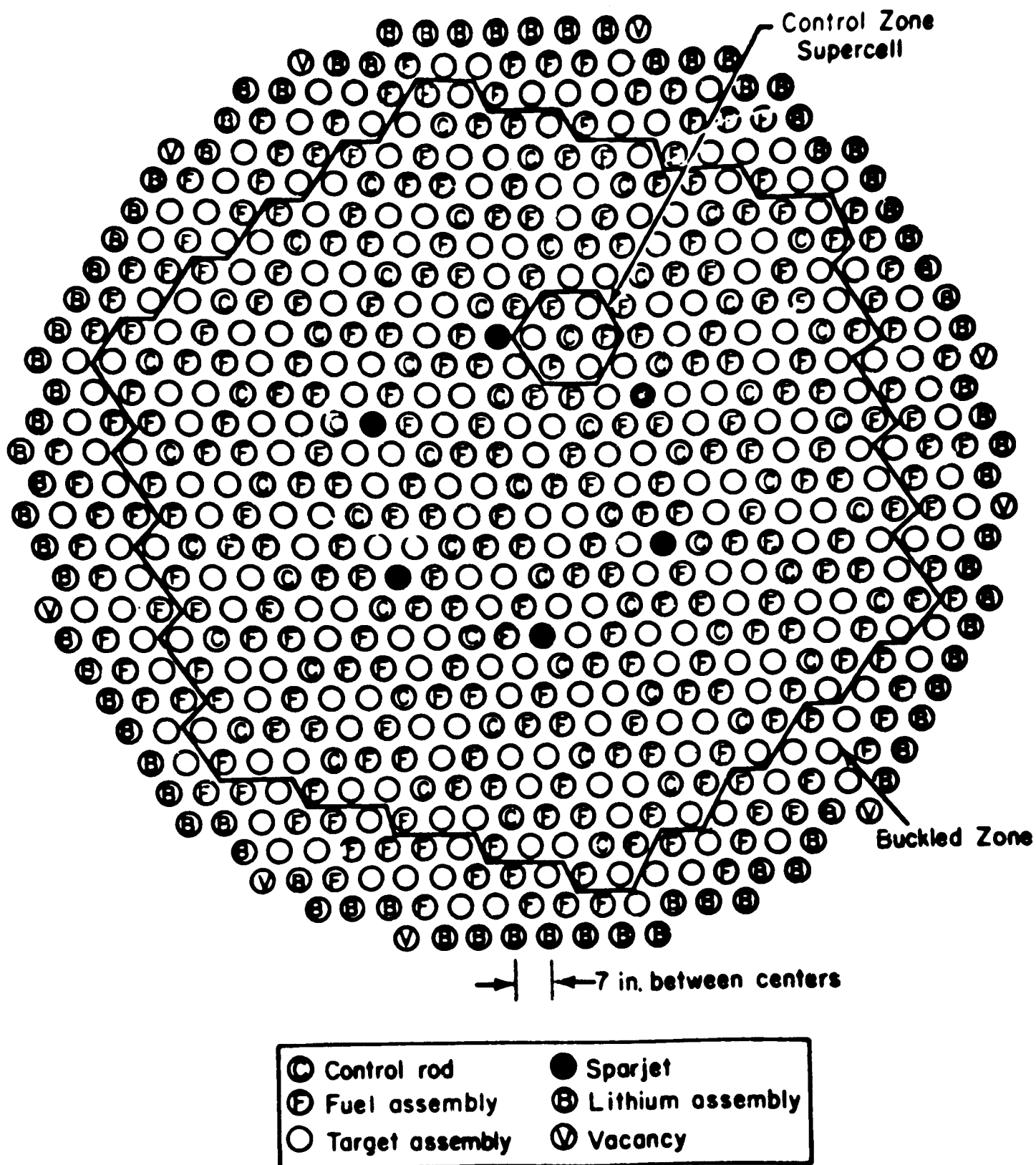


FIGURE 3

Face Map of a Typical Mixed Charge Lattice  
for a Savannah River Reactor

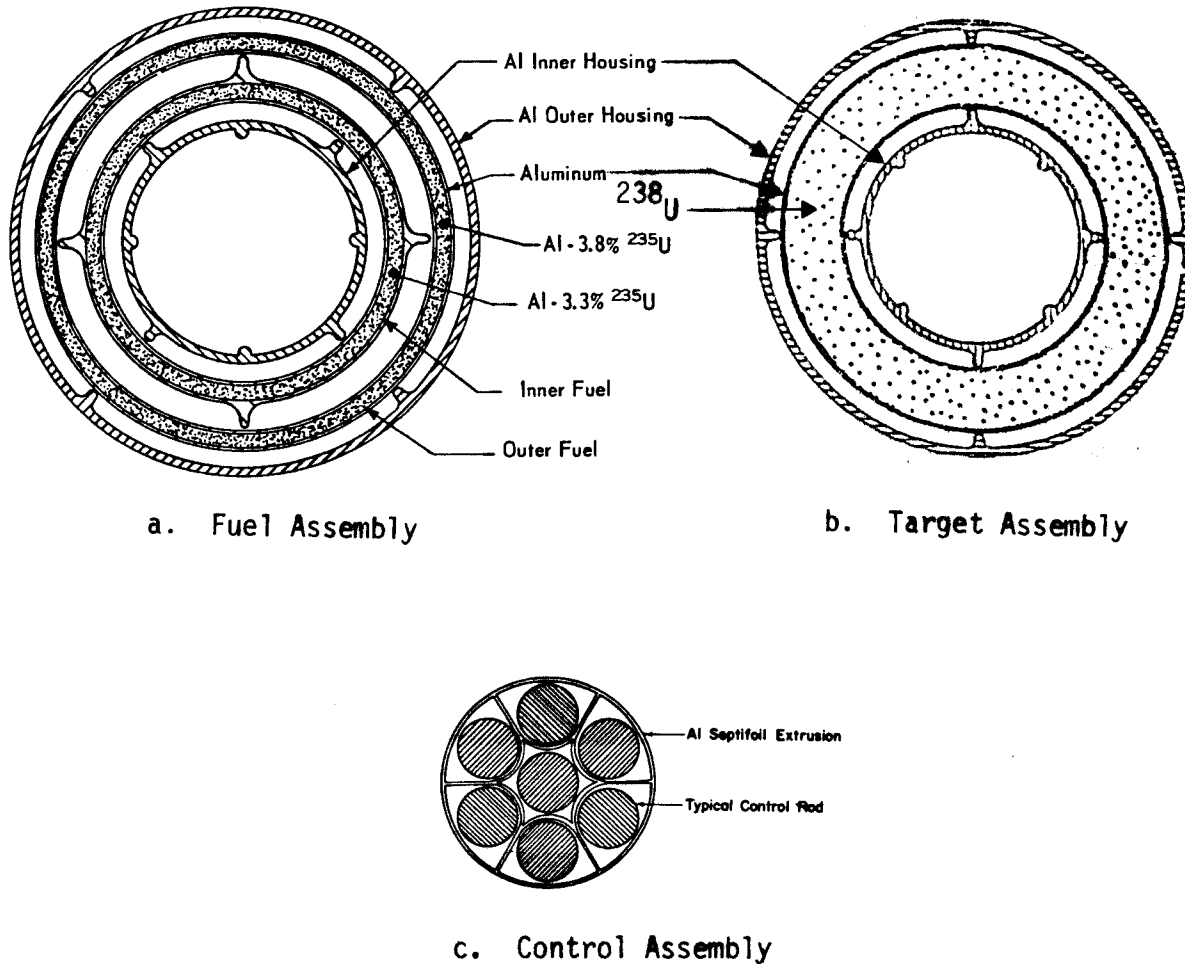


FIGURE 4  
Typical Savannah River Reactor Assemblies

reactor system. A vent is located above the reactor core but below the plenum, and maintains a low over-pressure on the reactor system. The vent system permits large resistance flow of  $D_2O$  from the reactor tank to an overflow system or to the process room above the reactor.

A high flux fuel assembly is shown in Fig. 4a. The fuel assembly consists of two annular shells to provide the maximum cooling area. The fuel is metal Al-U and uses >90% enriched  $^{235}U$ . However the concentration of the  $^{235}U$  in the Al-U fuel is only 3.3 - 3.8%. These fuel assemblies can be operated at very high power. Power is limited by the heat flux from the fuel surfaces and the limit is set so that the operating heat flux is no greater than about 60% of the heat flux required to cause burnout from film boiling. The dimensions of this fuel assembly are given in Table I. The coolant flow rates, velocities and pressures are given in Tables II-IV. The maximum power and heat fluxes are given in Tables V and VI while the maximum temperatures are given in Table VI. Notice that these reactors operate with very high flow rates and coolant velocities. They can operate very near to the critical heat flux because each assembly is individually instrumented and monitored. These reactors operate at very low temperature and pressures. This is because Al fuel is used. The choice of Al fuel comes from the desire to produce isotopically tailored Pu and other trans-uranic elements. This requires a very high flux and a short residence time for the fuel and target assemblies (~10 days). With so much fuel reprocessing required, the only economical choice is Al fuel. When these reactors make tritium the same type of assemblies are used, only in this case the reactors are operated at a lower power and for a much longer time, ~8 months. Hence Zircaloy fuel could be considered for such long irradiation

Table I (Fig. 4a)

High Flux Fuel Assembly, Dimensions

	<u>Dimension, inches</u>
Outer housing, OD	3.420
Inner housing, ID	3.300
Clad outer fuel, OD	3.020
Bare outer fuel, OD	2.960
Bare outer fuel, ID	2.796
Clad outer fuel, ID	2.736
Clad inner fuel, OD	2.354
Bare inner fuel, OD	2.294
Bare inner fuel, ID	2.108
Clad inner fuel, ID	2.048
Inner housing, OD	1.740
Inner housing, ID	1.640

Table II

Coolant Flow Rates

	<u>Flow, gpm</u>
Total	89,300
Fuel Assemblies	76,200
Single fuel assembly (average)	710
Outer annulus	242
Intermediate annulus	312
Inner annulus	151
Dead space	5
Control rods (in septifoils)	9,800
Single septifoil	135
Sparjets	3,300

Table III  
Coolant Velocities

	<u>Velocity, ft/s</u>
Fuel assembly	
Outer annulus	57
Intermediate annulus	70
Inner annulus	55
Bulk moderator in core	3-6

Table IV  
System Pressures

	<u>Pressure, psia</u>
Plenum	202
Above fuel tubes	155
Fuel tube $\Delta P$	130
Minimum inside bottom fitting	25
Bulk moderator outside bottom fitting	28.5
Gas above moderator	19.7

Table Va

Maximum Powers

	<u>Power, MW</u>
Total	735
Single fuel assembly	8.4
Per foot of fuel assembly	1.7
Per kg <sup>235</sup> U in fuel	177

Table Vb

Maximum Heat Flux and Minimum Burnout Safety Factor

	<u>Heat Flux, BTU/hr-ft<sup>2</sup></u>		<u>Burnout Safety Factor<sup>(b)</sup></u>
	<u>Operating<sup>(a)</sup></u>	<u>Burnout<sup>(a)</sup></u>	
Fuel			
Outer tube			
Outer surface	2,120,000	6,200,000	2.02
Inner surface	2,230,000	6,400,000	2.18 2.18
Inner tube			
Outer surface	2,120,000	6,400,000	q 2.11
Inner surface	2,080,000	5,900,000	1.84
Control rods			
Normal	220,000	1,200,000	4.2
Abnormal (largest rod, un- shadowed, at end of cycle)	580,000	1,200,000	1.6
Safety rod (inadvertently left in reactor)	270,000	430,000 <sup>(b)</sup>	1.6

(a) No hot spot factors applied

(b) Hot spot factors applied

Table VI  
Maximum Temperatures

	<u>Temperature, °C</u>
Inlet coolant	20
Fuel coolant outlet (single quadrant)	63
Fuel coolant outlet (calculated subchannel)	74
Reactor outlet	48
Bulk moderator	67
Fuel surface	
Outer tube	
Outer surface	128
Inner surface	128
Inner tube	
Outer surface	125
Inner surface	130
Fuel core (no allowance for oxide film)	
Outer tube	173
Inner tube	174
Control rod surface	
Normal	100
Abnormal (rod of largest cadmium diameter unshadowed at end of cycle)	170



times, but the practical constraints of developing two different reprocessing technologies prohibited this other choice.

The low temperature operation of these reactors precludes the conversion of the thermal energy to electricity.

The performance of these reactors (i.e., kg of T/MW<sub>th</sub>) is unavailable. However the upper limit of performance can be estimated. For purely thermal neutron spectra, the number of neutrons produced per <sup>235</sup>U atom destroyed is

$$\frac{\nu}{1+\alpha} = \frac{2.43}{1.18} = 2.06.$$

For more realistic neutron spectra the capture to fission ratio ( $\alpha$ ) is ~0.25 and the number of neutrons produced per <sup>235</sup>U atom destroyed is 1.94. Since one neutron is needed to carry on the chain reaction, this leaves 0.94 neutrons available to produce tritium. This is of course reduced by neutron leakage, absorption in the structure (Al) and absorption in fission products. Absorption in other uranium isotopes such as <sup>236</sup>U and <sup>238</sup>U can also be significant. The actual conversion ratio must therefore be less than 0.94 tritons per <sup>235</sup>U atom destroyed. If this analysis is carried out for <sup>233</sup>U and <sup>239</sup>Pu fuel as well, the results are those shown in Table VII. We see that both <sup>239</sup>Pu and <sup>233</sup>U will have a higher T conversion ratio than <sup>235</sup>U. In a hybrid system where T is produced in a production reactor, the hybrid will supply either <sup>239</sup>Pu or <sup>233</sup>U as the fissile fuel for the reactor rather than <sup>235</sup>U. Hence in the case of <sup>233</sup>U fuel we might expect the production reactor to perform as much as 30% better than it currently does. Assuming the energy released per fission is

190.0 for <sup>233</sup> U	
192.9 for <sup>235</sup> U	(MeV)
198.5 for <sup>239</sup> Pu	

Table VII  
Tritons Produced Per Fissile Atom Destroyed

	$\nu$	$\alpha_{th}$	$\alpha$	$\frac{\nu}{1+\alpha_{th}} - 1$	$\frac{\nu}{1+\alpha} - 1$	$\frac{\text{kg T}}{\text{MW}_{th}\text{-yr}}$
$^{235}\text{U}$	2.432	0.18	0.25	1.06	0.94	$4.8 \times 10^{-3}$
$^{233}\text{U}$	2.482	0.085	0.118*	1.29	1.22	$6.3 \times 10^{-3}$
$^{239}\text{Pu}$	2.874	0.33	0.46*	1.16	0.97	$4.8 \times 10^{-3}$

\* Assumed to be in same ratio as  $(\alpha/\alpha_{th})$  for  $^{235}\text{U}$ .

then the kilograms of tritium produced per  $\text{MW}_{\text{th}}$ -year is shown in the last column of Table VII.

It must be remembered that these are theoretical upper bounds on the tritium production. Actual production levels are likely to be about 10% less than these figures.

Another important consideration is the cost of the tritium producing facility. The cost of a Savannah River type reactor is given in Table VIII in 1979 dollars. A  $2200 \text{ MW}_t$  reactor costs \$715M or \$325/ $\text{kW}_t$  installed. This is to be compared to a cost of about \$300-350/ $\text{kW}_t$  installed for a power producing LWR. Hence we can assume that the tritium production reactor that produces no electricity costs about the same as a power producing LWR. At this cost, the price for tritium from such a facility would be ~\$20,000/gram.

### III.B. Hanford Graphite Moderated Production Reactors

The Hanford N-Reactor was initially designed for the production of Pu as well as power. However, there has also been experience with the production of tritium in this reactor. The conversion of the otherwise wasted heat substantially reduced the cost of the product. Steam is supplied to an adjacent utility-owned electric generating plant. The conversion capability was considered at its design stage in the event that future international disarmament agreements dictated that the production of reactor products for military uses be curtailed or stopped. Although there were rumors of placing the reactor on standby in 1977, it is still functioning in a dual-purpose capacity.

The reactor is basically of a simple design and consists of interlocking graphite bars acting as moderator and reflector, forming a stack of about 33-1/2 ft. high, 33 ft. wide, and 39-1/2 ft. long. The active core is about 25 ft. high, 23 ft. wide, and 35 ft. long. Figures 5 and 6

Table VIII

Cost of Savannah River Production Reactor

Capital Costs (2200 MW <sub>t</sub> )	\$460M
Discounted Cost at Startup (8 year construction at 10% discount rate)	\$660M
Initial Fuel Charge	<u>\$ 55M</u>
	\$715M
Annual Costs (Capital payback in 30 years)	\$ 76M
Purchased Power	\$ 36M
Cost of Tritium (\$/g)	\$19,500

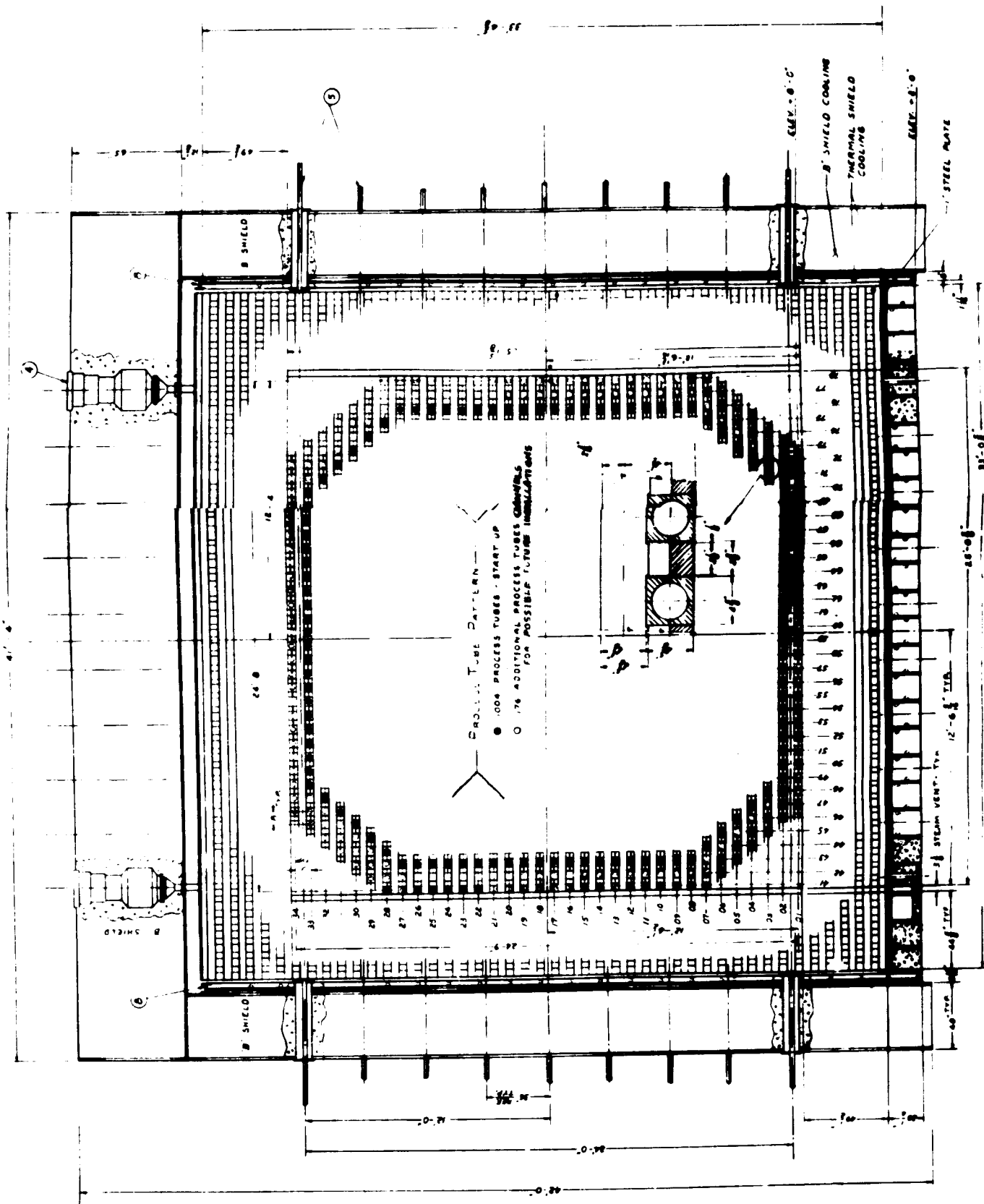


FIGURE 5 Front View of a Hanford Graphite Reactor

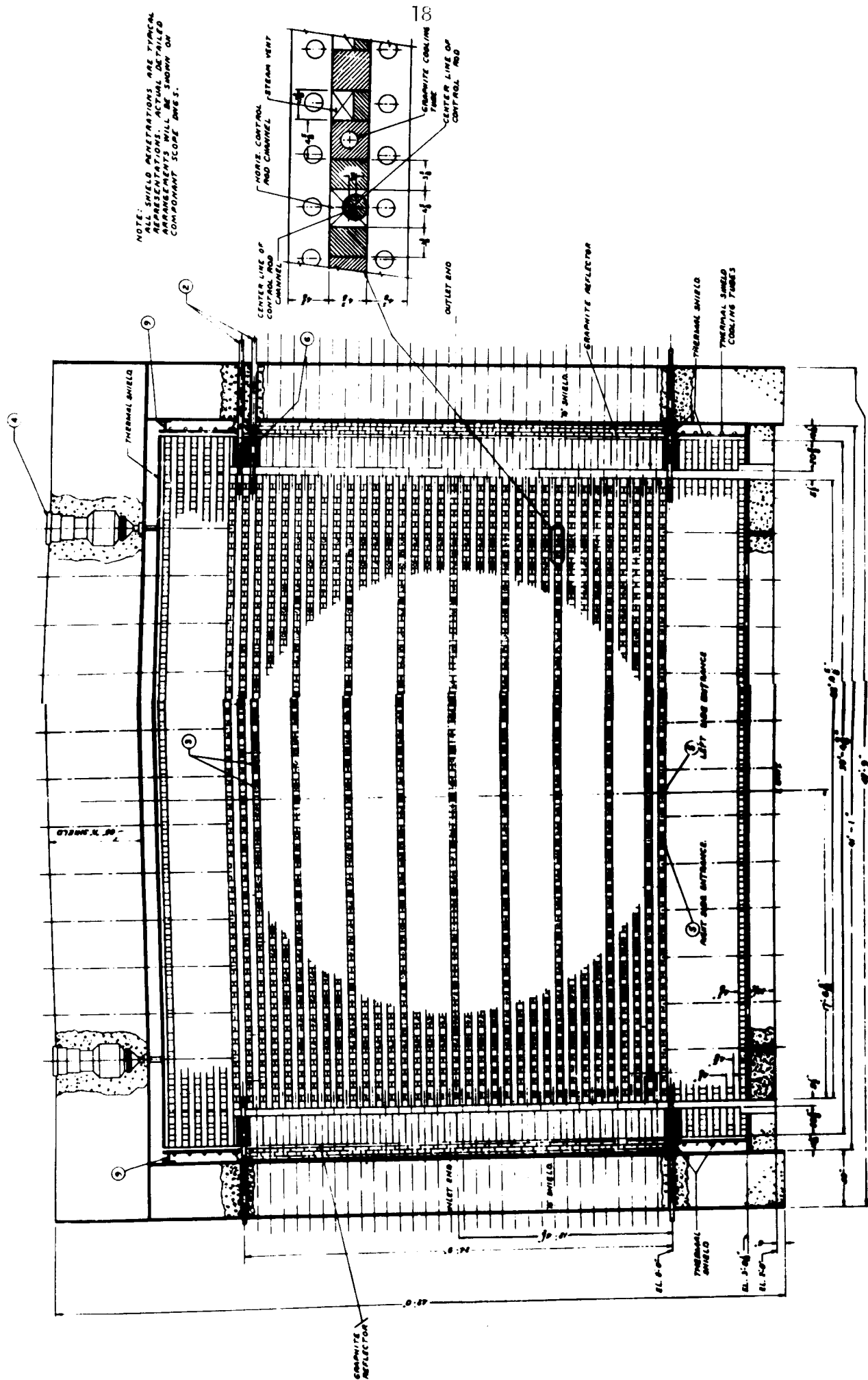


FIGURE 6 Side View of a Hanford Graphite Reactor

show face and side views of the reactor. The stacking pattern, as shown in Fig. 7, includes venting provisions to permit escape of the coolant which would be released in case a process tube ruptures. The vent channels have sufficient area to limit damage to the particular graphite bar in which the tube rupture would have occurred. There are a total of 1180 lattice units, 38 in the horizontal direction and 34 in the vertical direction, with 28 missing from each corner.

Gas plenums are placed between the moderator and the reflector graphite at the inlet and outlet of the stack as well as at both sides. A helium atmosphere is maintained normally, circulating through the active core from front to rear. The inert atmosphere prevents graphite oxidation, dries it when necessary, detects water and air leaks, prevents in-leakage of air by maintaining a positive pressure and provides a heat transfer medium for removal of moderator heat.

The stack, moderator and reflector are penetrated by 1003 process tube channels, extending from front to rear on an eight-inch horizontal by a nine-inch vertical lattice. A number of 86 horizontal control rod channels penetrate the graphite stack from side to side on a 32-inch horizontal by 36-inch vertical lattice. To achieve structural graphite temperature meeting contraction criteria, 640 moderator cooling channels enter the stack from side to side on a 16-inch horizontal by a 9-inch vertical lattice. Safety ball channels number 107, extending from top to bottom on a 32-inch by 32-inch spacing. These would be filled by 3/8-inch stainless steel boron containing balls (Fig. 8).

One-inch thick boron steel is used as the thermal shield material except at the inlet and outlet ends of the reactor where eight-inch thick cast iron blocks are used. Cooling tubes are welded to the boron steel plate. High density concrete is used as the primary shield on all sides

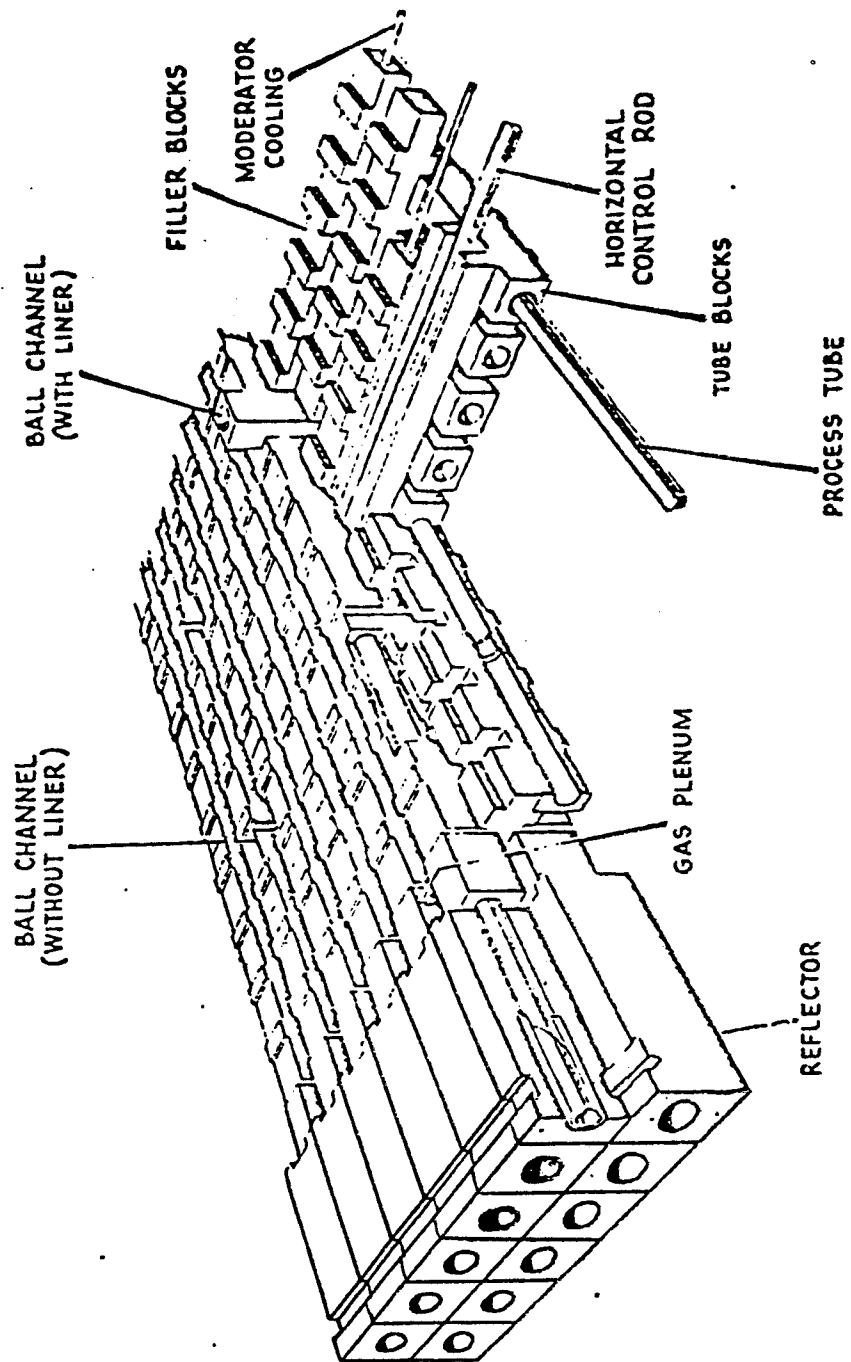
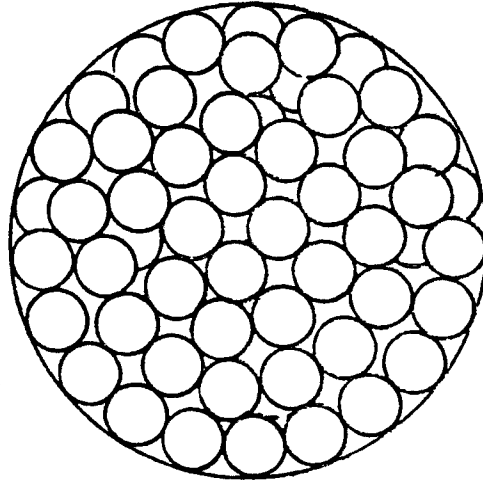


Fig. 7. Graphite Moderator Isometric





3.000" O.D. Cylinder

3/8" STAINLESS STEEL BALLS @ 1-1/2% BORON BY WEIGHT OR  
EQUIVALENT.

FIGURE 8

Balls Control System

of the reactor except at the bottom where ordinary concrete is used with thicknesses ranging from 40 to 72 inches. Personnel access is allowed only after shutdown. A biological shield surrounds the whole reactor structure and maintains radiation levels below 0.1 mr/hr in continuously occupied areas of the building.

Table VIII shows the lattice physics parameters for co-product tritium and Pu fuel and those of the standard fuel loading. Eta ( $\eta$ ), the ratio of neutrons born to thermal neutrons captured in fuel, is higher in the co-product fuel because of higher fuel enrichment (2.1%), although the difference is somewhat diminished by the buildup of Pu, which is a more pronounced effect in the standard fuel (9.947% enrichment). The fast fission factor ( $\epsilon$ ) is lower in the co-product fuel because of the reduction in uranium content. The resonance escape probability ( $p$ ) is higher in the co-product fuel for the reduced U content. The thermal utilization ( $f$ ) of the co-product fuel is lower because absorptions in the target are considered parasitic for reactivity calculations — were these absorptions to be considered as fuel absorptions, the co-product,  $f$ , would increase to about 0.92, or three per cent higher than the standard fuel. The Fermi age ( $\tau$ ) increases in the co-product case primarily because the area of the coolant passages is reduced by 15 per cent, reducing the total slowing down power of the lattice. The thermal diffusion area ( $L^2$ ) is decreased because of the increased blackness to thermal neutrons of the co-product fuel. This discussion implies that for a system dedicated to tritium production higher enrichments will be needed, substantially changing the design parameters to the extent of needing a new design of the reactor.

Table IX shows the operating parameters and data of the system. The riser's configuration is shown in Fig. 9. Demineralized ordinary water is used as a coolant. For a maximum credible accident where all water is

Table VIII    Lattice Physics Parameters for Standard and Coproduct Operational Modes of the N-Reactor

---



---

<u>Lattice Physics Parameters</u>				
<u>Parameter</u>	<u>Cold</u>		<u>Hot, Operating</u>	
	<u>Standard</u>	<u>Coproduct</u>	<u>Standard</u>	<u>Coproduct</u>
$\eta$	1.400	1.651	1.352	1.572
$\epsilon$	1.039	1.029	1.040	1.030
$p$	0.836	0.866	0.820	0.848
$f$	0.866	0.736	0.893	0.748
$\tau$ (cm <sup>2</sup> )	395	433	41	448
$L^2$ (cm <sup>2</sup> )	139	130	161	152
$k_\infty$	1.053	1.082	1.029	1.028
$k_{\text{eff}}$	1.033	1.060	1.008	1.005
$\rho$ , mk	32.3	56.3	7.9	5.2

---



---

Table IX Operating Data and Physical Parameters  
of the N-Reactor

	<u>4800 MW</u>	<u>4000 MW<sup>(a)</sup></u>
<u>OPERATING DATA</u>		
Inlet Process Water Temperature - °F	390	386
Maximum Outlet Process Water Temperature - °F	567	535
Target Temperature - approximate	process water temperature	
Maximum Fuel Temperature - °C	548	492
Average Fuel Temperature - °C	434	396
Average Pressure Drop Across Fuel Column - psi	177	177
Rear Riser Pressure - psia	1500	1500
Process Water Flow per Channel - #/hr	94,400	94,400
Total Process Water Flow - Million #/hr	94.7	94.7
Core Length - ft	31	31
Maximum Tube Power - MW (full load)	5650	4700
Maximum Tube Power - MW (transition)	5940	4950
Heat Flux (Driver) - Btu/hr/sq ft		
Inner Surface	785,000	659,000
Outer Surface	683,000	571,000
Heat Flux (Target)	Negligible	
Maximum Heat Flux/Burnout Heat Flux	<0.33	<0.23
Tube Maximum Power Density - kW/ft	240	208
Reactor Average Power Density - kW/ft	151	131
Gas Volume Ratio in Target	3.5	3.4
Steam Pressure - psia	150	150
<u>PHYSICAL PARAMETERS</u>		
Shutdown Margin (Rods Only) - mk	17	20
Control Rod Strength - mk	77	77
Ball System Strength - mk	62	62
Maximum Cold Xenon-Free Reactivity - mk	60	57

(a) Fuel design capable of operation at reactor power level of 4800 MW.

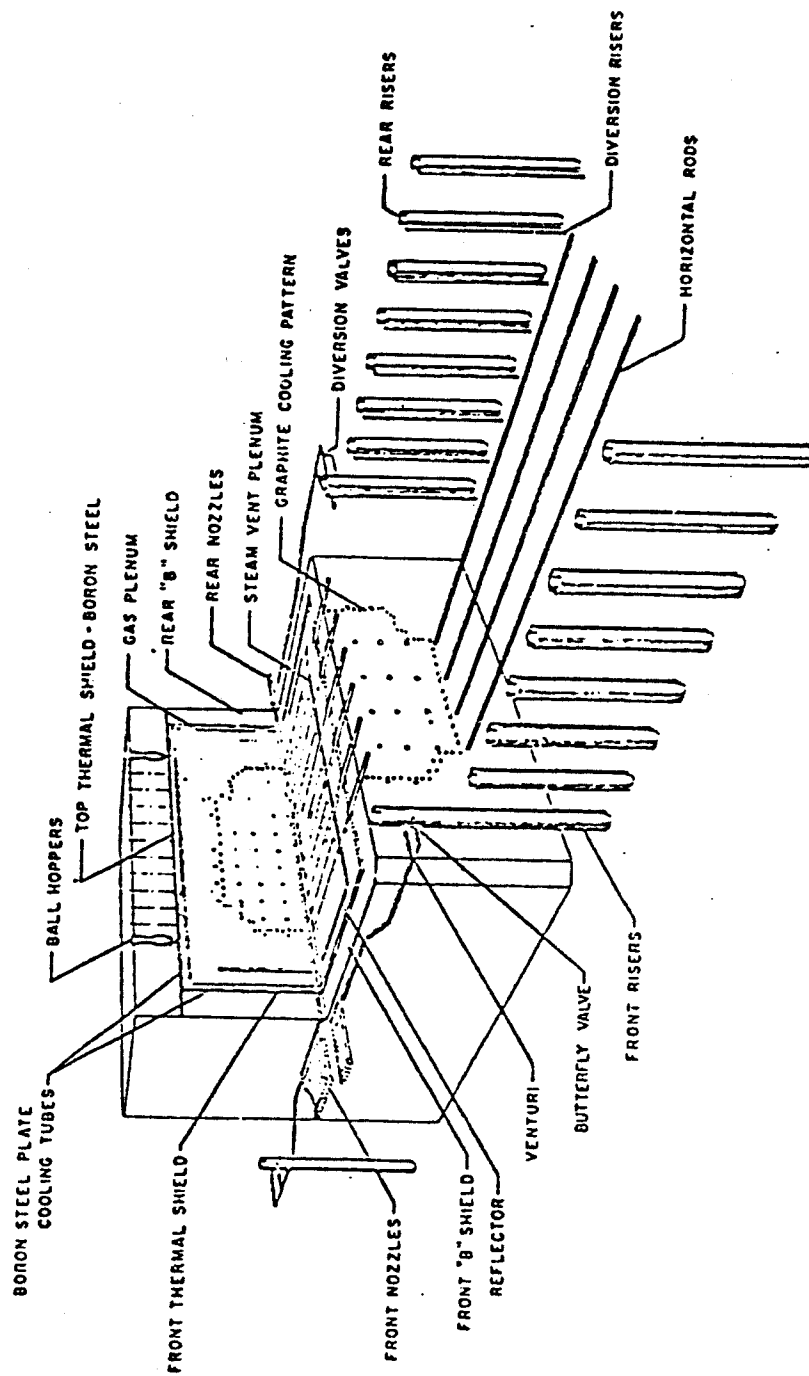
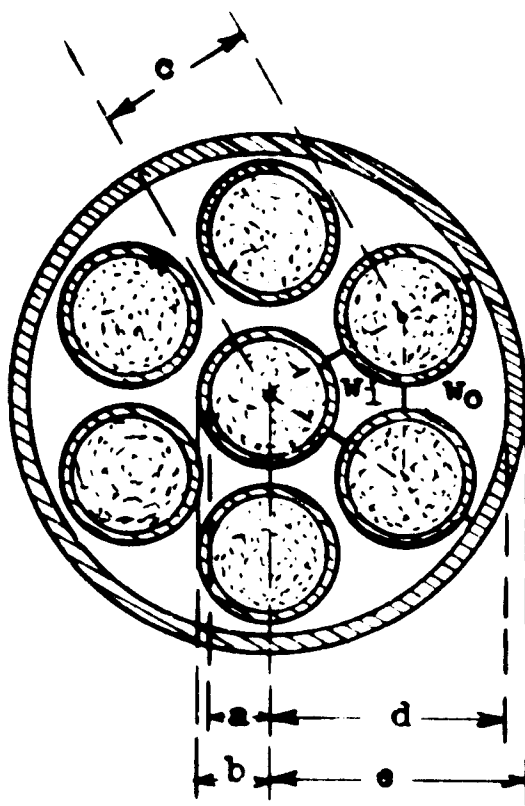


Fig. 9. Configuration of the 105-N Reactor

lost to the reactor, the graphite system removes fission product decay heat and has a backup source of raw water. The coolant system is operated at low temperatures and pressures to permit the use of aluminum together with Zircaloy-2 tubing. A maximum outlet water temperature of 535°F is attained with a maximum fuel temperature of 492°C.

Driver and fuel elements are shown in Figure 10 and consist of a seven-rod cluster element. Two types of clusters are used. Cluster A, for driver fuel, is composed of slightly enriched uranium with Zircaloy-2 cladding. Cluster B, for target fuel, is composed of natural uranium with Al cladding, for Pu production. Normal operation enrichment of the driver elements is 9.947%, but for the co-production case, it is 2.1%. The discharge fuel enrichment is 0.68 - 0.74 per cent. The fuel pile loading is 350-516 tons and the maximum fuel element length is 35-inches. The pressure tubes are made of Zircaloy-2 with 2.7-inch inside diameter and 0.25-inch minimum wall thickness.

There are two types of control rods, as shown in Figs. 11 and 12. The first type is a boron control and safety rod composed of boron carbide and aluminum. The second is a lithium-aluminum control rod. Both are enclosed in a steel sheath. Tritium will be produced in the Li-Al rods. In the studies conducted on co-production of tritium and plutonium, Li-Al alloys with 3 wt% Li in Al and 41% enriched in  $^6\text{Li}$ , as well as Li-Mg alloys were considered. Li silicates, aluminates and aluminosilicates were also studied. Double Zr and Al canning is used where the Al acts as an efficient barrier to the tritium produced from the  $^6\text{Li} + {}_0^1\text{n} \rightarrow \text{T} + \alpha$  reaction.



Cluster Dimensions

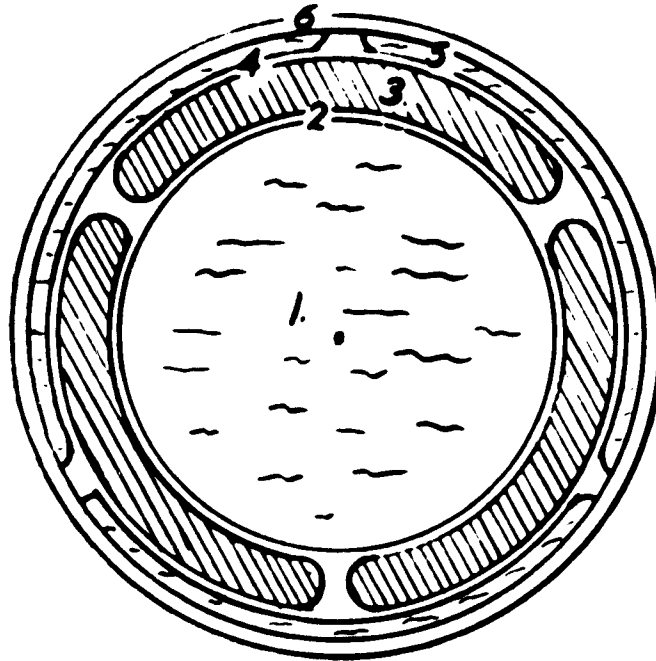
Cluster	a (in.)	b (in.)	c (in.)	d (in.)	e (in.)
A	.250	.298	.648	.997	1.0605
B(771)	.322	.352	.851	1.35	1.60

Cluster A: Natural uranium, 28 aluminum tubes.  
7-1/2 inch lattice

Cluster B: 0.95% enriched uranium, zircaloy-2  
tubes. 8-3/8 inch lattice assumed  
in calculation.

FIGURE 10

Driver and Target Cluster Configurations



BORON CONTROL & SAFETY ROD

<u>Region</u>	<u>Material</u>	
1	Water	Radius = 0.8835"
2	Aluminum	Thickness = 0.065
3	Boron Carbide	0.218
4	Aluminum	0.065
5	Water	0.078
6	Steel	0.065

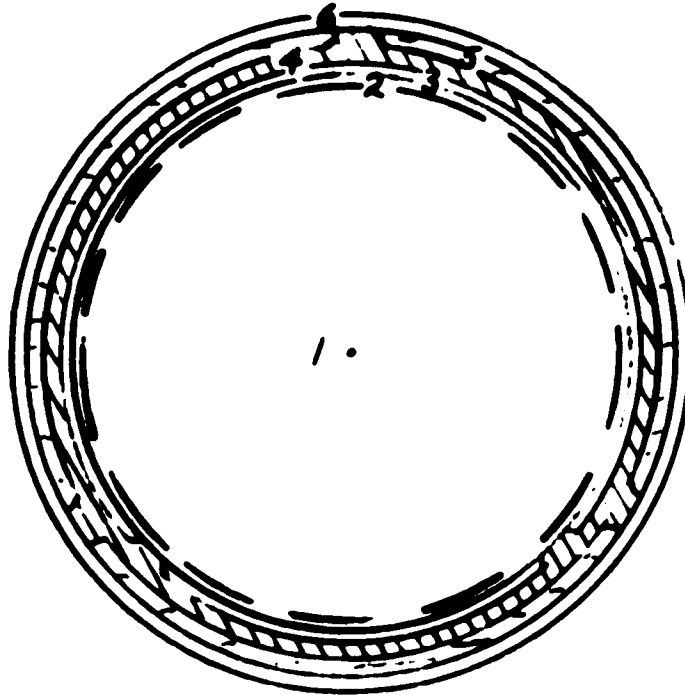
HCR Channel Dimensions

At tube block	4-5/8" x 4-3/8"
At filler block	4-5/8" x 6-11/16"
Average dimensions	4-5/8" x 5-3/8"

FIGURE 11

Boron Control and Safety Rod





LITHIUM ALUMINUM CONTROL ROD

<u>Region</u>	<u>Material</u>	
1	Lithium Aluminum	Radius=1.025"
2	Aluminum	Thickness=0.040
3	Water	0.102 *
4	Aluminum	0.065
5	Water	0.078
6	Steel	0.065

\*After irradiation, which results in swelling of lithium aluminum slug, water thickness will be reduced to 0.078".

FIGURE 12

Li-Al Control Rod

Prototype lithium aluminate target elements shown in Figs. 13 and 14 were irradiated in the N-Reactor. These elements consisted of 24-inch long Zircaloy-2 cans, 1.316-inch OD, having either 0.03- or 0.095-inch walls, each containing two aluminum-canned ceramic cores. The Al cans were approximately 1.25-inch OD, approximately 12-inches long and had a 0.050-inch wall. The  ${}^6\text{Li}/\text{Li}$  weight per cent at 78% bulk density was: 2.84, 1.59, 6.43 for the base, spike and poison (natural lithium) compositions, respectively.

Steam pressures of 75-500 psia were achieved. Steam is fed to turbine generators of 200-300 MWe each for a generating total capacity of 300-900 MWe net.

Table X shows the economic parameters for the operation of the plant from a study on its conversion to production of Pu with  ${}^{240}\text{Pu}$  content. The important observation is that the steam credits reduce the product cost by about  $\frac{20.00 - 14.93}{20.00} \times 100 = 25.35\%$ , a substantial savings. A Savannah River plant is at a disadvantage from this point of view, since it does not produce power and even needs to buy external power for its reactor's operation.

A study has considered the conversion to co-production of Pu and tritium and tritium has actually been produced in it for a short period around 1967. Table XI shows its production data. For an operation at  $4800 \text{ MW}_{\text{th}}$ , 815 kg of Pu can be produced per year together with 6.25 kg of tritium. This amounts to  $1.3 \times 10^{-3} \text{ kg/MW}_t \cdot \text{yr}$ .

Assuming that all the produced Pu could have been replaced by tritium, this amounts to (Av is Avogadro's Number):

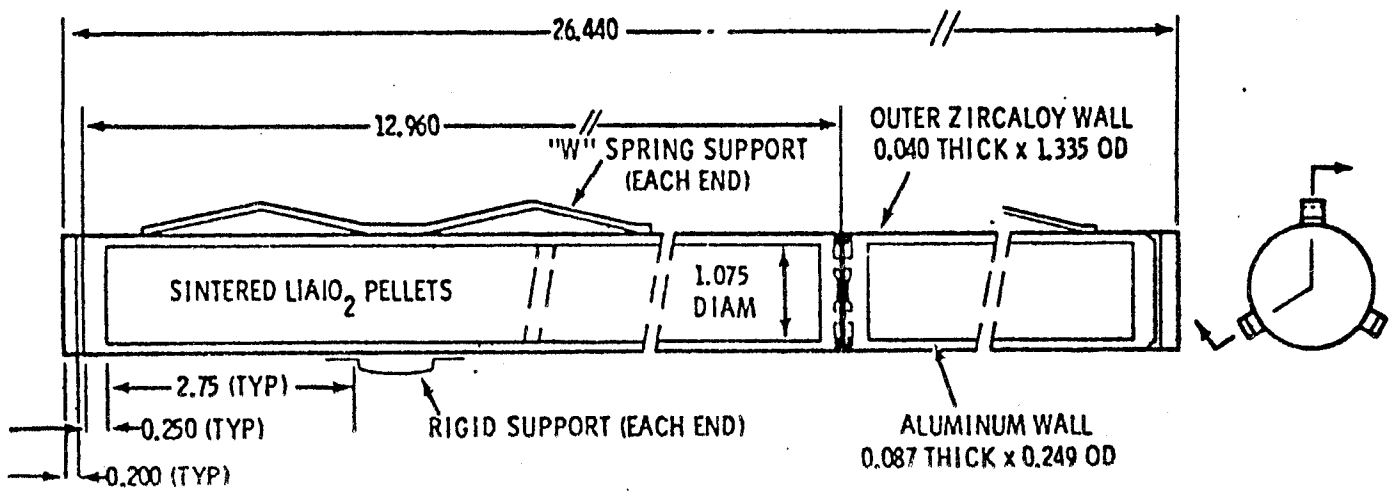


Fig. 13. Cross Section of Coproduct Target Element

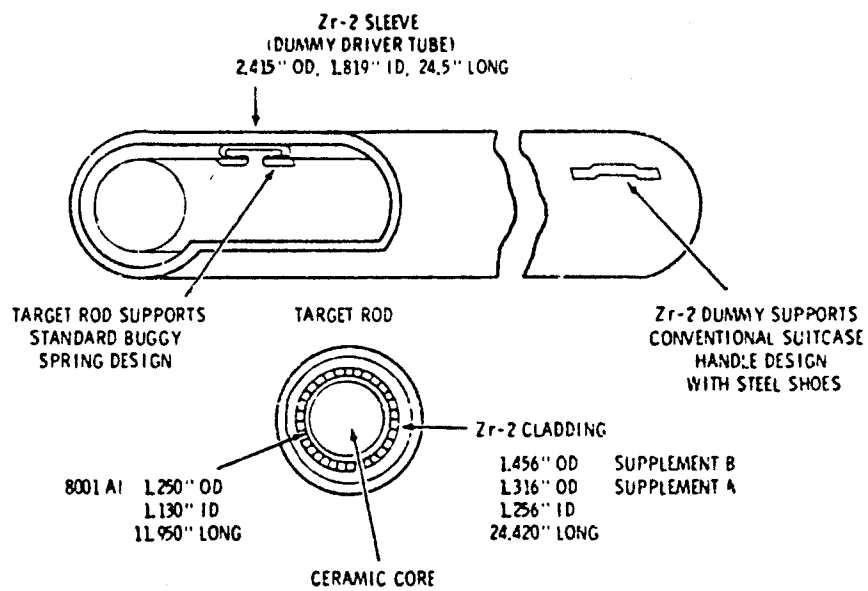


Fig. 14. Coproducer Target Test Element

Table X  
Economic Parameters of the N-Reactor  
 (1972 Projected Figures)

---

Reactor Production:

Power Level, MW <sub>th</sub>	4800
Burnup, MWD/T	3000
Pu generated, kg	1028
Uranium Throughput, Tons/yr	498

Production Costs (in \$ Million)

Off-site Costs

Uranium	1.992
---------	-------

On-site Costs

Fuel Fabrication	3.595
Irradiations	6.130
Separations	1.404
Burnout Costs	7.438
Total Product Cost	20.559
STEAM CREDITS	(5.208)
Net Product Costs Without Np Credits	15.351
Unit Costs <u>Before</u> Steam Credits, \$/gm	20.000
Unit Costs <u>After</u> Steam Credits, \$/gm	14.930
% <sup>240</sup> Pu Content of Product	15.400

---

Table XI Data for Combined Tritium-Plutonium  
Production in the N-Reactor

	<u>4800 MW</u>	<u>4000 MW<sup>(a)</sup></u>
<u>PRODUCTION DATA</u>		
Fuel Enrichment - % U-235		
In	2.10	2.10
Out	1.91	1.91
Fuel Exposure - MWD/T	1675	1664
Tons Uranium Per Year	878	737
No. Fuel Assemblies Per Year (average length - 24")	60,140	50,480
Conversion Ratio - g Pu equiv/MWD		
Plutonium	0.554	0.548
Tritium	0.340	0.340
Production		
Plutonium - kg/yr	815	672
Tritium - kg/yr expressed as Pu equiv	500	417
Total Production - kg Pu equiv/yr	1315	1089
Tritium - kg/yr	6.25	5.2

---

(a) Fuel design capable of operation at reactor power level of 4800 MW.

---

$$815 \text{ kg Pu} \times 10^3 \frac{\text{g Pu}}{\text{kg Pu}} \times \frac{A_v}{239} \frac{\text{atom Pu}}{\text{g Pu}} \times 1 \frac{\text{atom T}}{\text{atom Pu}}$$

$$\times \frac{3}{A_v} \frac{\text{g T}}{\text{atom T}} \times 10^{-3} \frac{\text{kg T}}{\text{g T}} = 10.23 \text{ kg T/yr},$$

which is equivalent to  $2.13 \times 10^{-3} \text{ kg T/MW}_e\text{-yr}$ . In the last case, higher enrichments may have to be used with the fissile fuel supplied by the fusion reactor, but we may obtain a total of  $2.13 \times 10^{-3} + 1.3 \times 10^{-3} = 3.43 \times 10^{-3} \text{ kg T/MW}_e\text{-year}$ , which is much better than converted LWRs. This is not astonishing in view of the large conversion ratio of such a system in spite of its low fuel burnup of 1675 MWD/T.

The production values are less than those of the Savannah River reactors but this reactor produces electricity as well as tritium. Although the design of the N-Reactor is outdated and better designs may be achievable today, these data are still an important demonstration of the fact that tritium can be successfully manufactured in a power producing reactor. In this case, only about a 30% penalty is paid in the production rates. This figure might be used as a rough rule of thumb when comparing electricity producing and non-electricity producing tritium production reactors.

### III.C. Light Water Reactors and Modified Light Water Reactors

The major source of tritium in LWRs is from ternary fission. This amounts to about  $1.18 \times 10^{-3} \text{ kg/MW}_e\text{-year}$ . This would be recovered in the fuel reprocessing plant. Some tritium is produced in burnable poison pins, but these are only included in the core during the first cycle of operation. Hence, unless the LWR reactor is modified in a significant way, it does not produce very much tritium, without reprocessing the fuel. If the reactor is considerably modified by the inclusion of  $^6\text{Li}$  pins in the core and a consequent power derating, then the tritium production can be increased to  $1 \times 10^{-2} \text{ kg/MW}_e\text{-yr}$ .



#### IV. Liquid Metal Fast Breeder Reactors

Liquid metal fast breeder reactors may be able to produce significant amounts of tritium in addition to sustaining their own fissile fuel inventory. Such a reactor may be desirable for producing the initial tritium inventories for hybrids or may be operated in tandem with the hybrid. Survey calculations<sup>(3)</sup> have been performed for a number of different variations of the standard LMFBR. These have involved the replacement of the sodium coolant with natural Li and 100%  $^7\text{Li}$ . In another set of calculations the radial blanket has been replaced with a tritium breeding blanket. The use of  $^{233}\text{UO}_2$  fuel rather than  $\text{PuO}_2$  fuel was also investigated. Finally,  $\text{Li}_2\text{O}$  was used in the radial blanket rather than lithium metal.

##### Model for the Calculations

The model for the calculations has been prepared by ANL and is completely described in reference 4. The most important characteristics are:

- mixed oxide fuel
- ~1250 MW<sub>e</sub> clean LMFBR
- two-zone core without control rods in control rod position
- core height 40 in.
- core radius 69.5 in.
- core volume 9950 liters
- blanket and reflector regions included
- volume fraction:

fuel	41%
total sodium	38%
total structure	21%

Fig. 15 shows the geometry with dimensions and interval numbers. Table XII contains the complete specification for the reactor mixtures.

#### Replacement of Sodium by Lithium

For the calculations of the Li atom number densities the following formula was applied:

$$\frac{A_d A}{\rho} = \text{constant}$$

$A_d$  Atom number density

$A$  Atomic mass of material

$\rho$  Material density .

Following input data was used

- sodium

Temperature 1100 K

Density 0.7533 g/cm<sup>3</sup>

- lithium

Temperature 500 K

Density 0.4793 g/cm<sup>3</sup>

composition of natural Li

Li<sup>6</sup> 7.42%

Li<sup>7</sup> 92.58%

From this data a multiplication factor results:

$$F_A = \frac{A_D^{\text{Li}}}{A_D^{\text{Na}}} \approx 2$$

The data of Table XIII have been applied for the lithium isotopes. For the fuel, a temperature of 500 K has been taken.

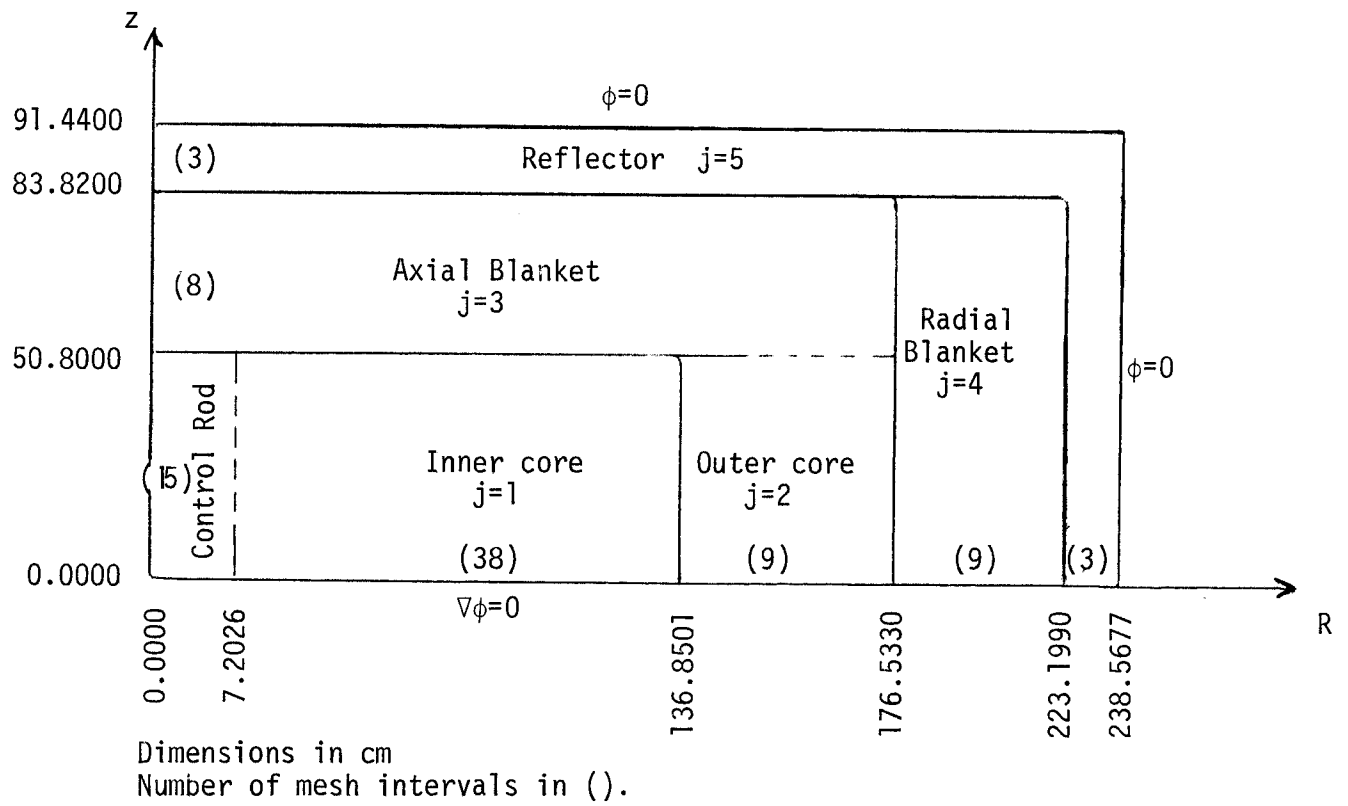


FIGURE 15

Geometry of LMFB International Comparison Calculational Model.

Table XII Compositions and Associated Broad Group Cross Section Sets\*

Cross Section Set Ident.**	Inner Core			Outer Core			Axial Blanket			Radial Blanket	Refl. G	Boron Control Rod			Na Filled Control Rod Position	Hot Fuel Cross Sections***								
	Na In		Na Void	Na In		Na Void	Na In		Na Void			Na In		Na Out <sup>†</sup>		Inner Core		Outer Core						
	A	B		C	D		E	F				G	A	B		Na In	Na Void	A <sup>H</sup>	Na In	Na Void	C <sup>H</sup>	Na In	Na Void	D <sup>H</sup>
Na 16 <sub>O</sub>	9.6673 <sup>-3</sup>	0.0000		9.6673 <sup>-3</sup>	0.0000		9.6673 <sup>-3</sup>	0.000		6.1299 <sup>-3</sup>	9.6673 <sup>-3</sup>	8.5022 <sup>-3</sup>		17.7718 <sup>-3</sup>										
Fe	17.3293 <sup>-3</sup>			17.3299 <sup>-3</sup>			17.8922 <sup>-3</sup>			27.1562 <sup>-3</sup>														
Ni	11.2693 <sup>-3</sup>			11.2693 <sup>-3</sup>			11.2693 <sup>-3</sup>			8.7384 <sup>-3</sup>	13.9943 <sup>-3</sup>	17.7433 <sup>-3</sup>		10.0239 <sup>-3</sup>										
Cr	2.2435 <sup>-3</sup>			2.2435 <sup>-3</sup>			2.2435 <sup>-3</sup>			1.7397 <sup>-3</sup>	29.5122 <sup>-3</sup>	3.5324 <sup>-3</sup>		1.3228 <sup>-3</sup>										
	3.2840 <sup>-3</sup>			3.2840 <sup>-3</sup>			3.2840 <sup>-3</sup>			2.5464 <sup>-3</sup>	9.6621 <sup>-3</sup>	5.1706 <sup>-3</sup>		2.8795 <sup>-3</sup>										
Mo	0.2339 <sup>-3</sup>			0.2339 <sup>-3</sup>			0.2339 <sup>-3</sup>			0.1814 <sup>-3</sup>	0.2239 <sup>-3</sup>	0.3683 <sup>-3</sup>		0.0218 <sup>-3</sup>										
Mn	0.2842 <sup>-3</sup>			0.2842 <sup>-3</sup>			0.2842 <sup>-3</sup>			0.2203 <sup>-3</sup>	0.3607 <sup>-3</sup>	0.4474 <sup>-3</sup>		0.2387 <sup>-3</sup>										
235U	0.0155 <sup>-3</sup>			0.0149 <sup>-3</sup>			0.0184 <sup>-3</sup>			0.0279 <sup>-3</sup>														
238U	7.6440 <sup>-3</sup>			7.3256 <sup>-3</sup>			9.0634 <sup>-3</sup>			13.7561 <sup>-3</sup>														
239Pu	0.7704 <sup>-3</sup>			0.9868 <sup>-3</sup>																				
240Pu	0.2208 <sup>-3</sup>			0.2828 <sup>-3</sup>																				
241Pu	0.1165 <sup>-3</sup>			0.1497 <sup>-3</sup>																				
242Pu	0.0279 <sup>-3</sup>			0.0358 <sup>-3</sup>																				
10B												14.8031 <sup>-3</sup>												
12C												7.5013 <sup>-3</sup>												
11B												14.8031 <sup>-3</sup>												

\* Number densities in atoms/barn-cm.

\*\* Broad group cross sections are obtained by collapsing over the spectra appropriate for the listed compositions.

\*\*\* The "hot fuel" cross section sets are generated with the temperatures of 235<sub>U</sub>, 238<sub>U</sub>, 239<sub>Pu</sub>, 240<sub>Pu</sub>, 241<sub>Pu</sub>, and 16<sub>O</sub> set of 2200 K while the temperature of all other isotopes is set at 1100 K.

† Note that the control rod composition contains sodium even though the surrounding core is sodium voided.

Table XIII    Li Atom Densities

Coolant	Number density          atoms/barn-cm	
	Core mixtures Ax. Blanket Reflector	Rad. Blanket
100 % Li <sup>7</sup>	19.335 10 <sup>-3</sup>	12.260 10 <sup>-3</sup>
92.58 % Li <sup>7</sup>	17.900 10 <sup>-3</sup>	11.350 10 <sup>-3</sup>
7.42 % Li <sup>6</sup>	1.435 10 <sup>-3</sup>	0.910 10 <sup>-3</sup>

### Changes in Fuel Compositions

Replacement of sodium by lithium results in a decrease of reactivity for the reactor considered. This is caused by the better moderation, leading to a softer neutron spectrum and in the case of  $\text{Li}^6$  by the strong absorption.

Criticality was maintained by increasing the fissile material at constant fuel inventory. The following formulae were applied:

$$\text{- Reference Reactor } \frac{U}{Pu} = a$$

New Pu-Inventory  $Pu'$

New U Inventory  $U'$

$$\text{- Lithium Reactor } \frac{Pu'}{Pu} = q > 1$$

For  $U + Pu = \text{constant}$

$$\frac{U'}{U} = \frac{a + 1 - q}{a}$$

In all mixtures the same ratios  $\frac{Pu'}{Pu}$  and  $\frac{U'}{U}$  were used. A very crude search to criticality was carried out. No power shape optimization was done. For the natural Li coolant the ratio  $\frac{Pu'}{Pu} = 1.4$  was necessary with  $\frac{U'}{U} = 0.95$ .

The 100%  $\text{Li}^7$  coolant needed  $\frac{Pu'}{Pu} = 1.05$ ,  $\frac{U'}{U} = 0.997$ . In both cases the resulting  $k_{\text{eff}}$  was about 2-3% greater than 1. This result was also obtained for the reference reactor with the applied nuclear data.

### Applied Nuclear Data

The calculations were performed with the 26-Group KFKINR-Set, commonly used at Karlsruhe for fast reactor design calculations. Only for the materials  $\text{Li}^6$  and  $\text{Li}^7$  the scalar group constants were recalculated. With the code BRIGITTE, ENDF/B-III data has been transferred to KEDAK-format and processed to group constants, within the KAPROS-System,

by the procedure GRUCON.

### Calculation Methods

The production rate calculations were performed with 26-group, two-dimensional diffusion calculations as specified for the benchmark calculations (accuracy 1%). In the KAPROS system a time-saving procedure DISCON was utilized. The energy independent fission source for the two-dimensional diffusion calculation with the KAPROS procedure DIXY is estimated with increasing energy group number. Group collapsing and succeeding DIXY runs are organized by the procedure DIXCON. Also plots of condensation spectra and of flux traverses are produced.

Fig. 16 and 17 show condensation spectra for natural lithium and 100% enriched  $\text{Li}^7$ . We may observe the strong influence of the  $\text{Li}^6$  absorption at low energies in the natural lithium case.

Fig. 18 and 19 show axial and radial traverses of the flux distributions with 100%  $\text{Li}^7$ . Represented are the total flux and the first 4 groups of the 26-group system. The normalization is calculated for  $\sim 3000 \text{ MW}_{\text{th}}$ . The calculation of the reaction rates in the reactor is performed with the procedure DIXY (Module DXEVA).

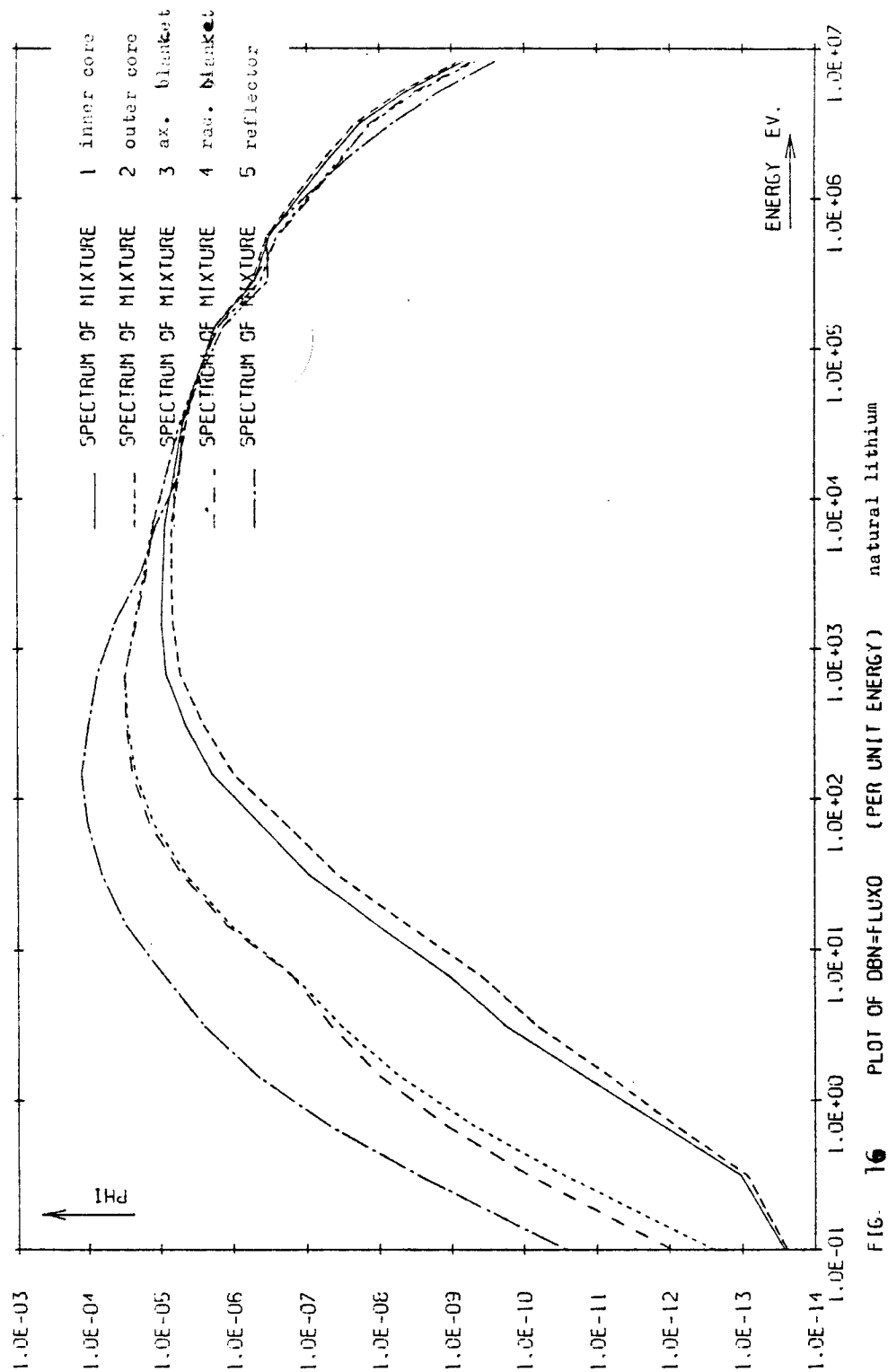
### Results

The procedure DIXY calculates the integral

$$i_{R_y}^x = \frac{1}{4\pi} \int_{(R)} \int_{\Delta E_i} \sigma_y^x(\vec{r}, E) \phi(\vec{r}, E) d\vec{r} dE$$

with

$$\int_{(R)} \int_{(E)} v \Sigma_f(\vec{r}, E) \phi(\vec{r}, E) d\vec{r} dE = 1$$





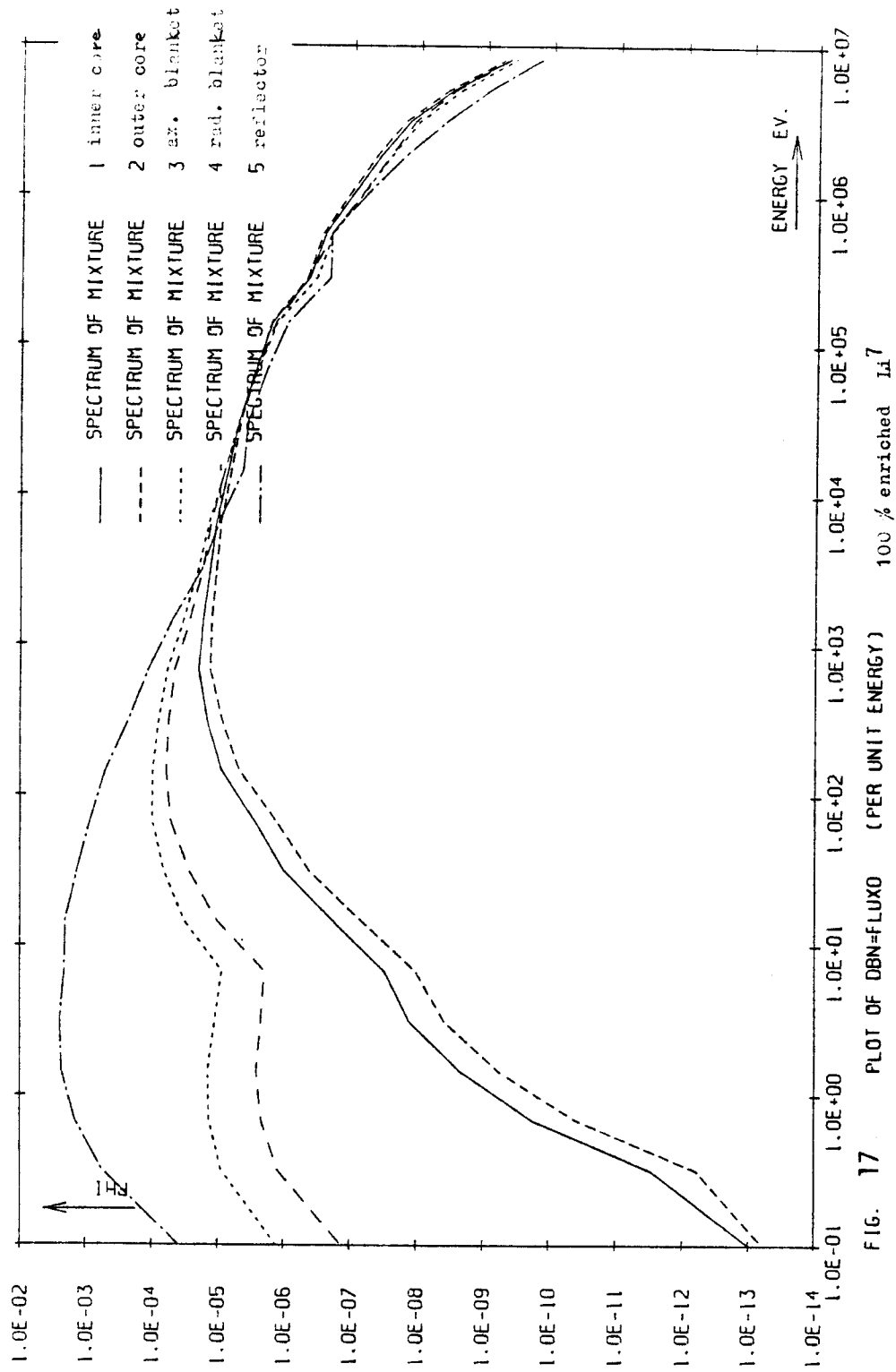
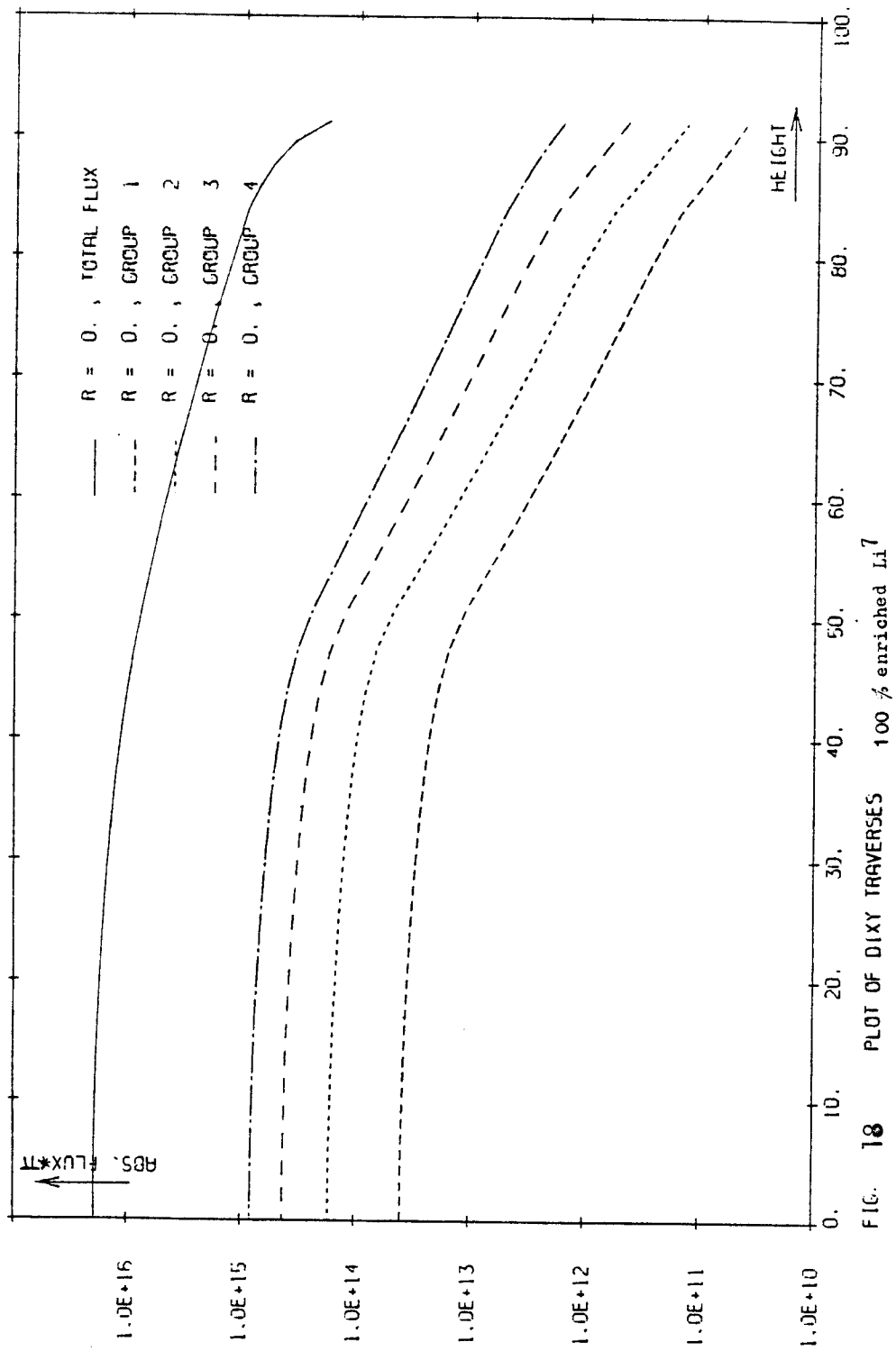


FIG. 17

FIG. 18 PLOT OF DIXY TRAVERSES 100% enriched  $Li^7$

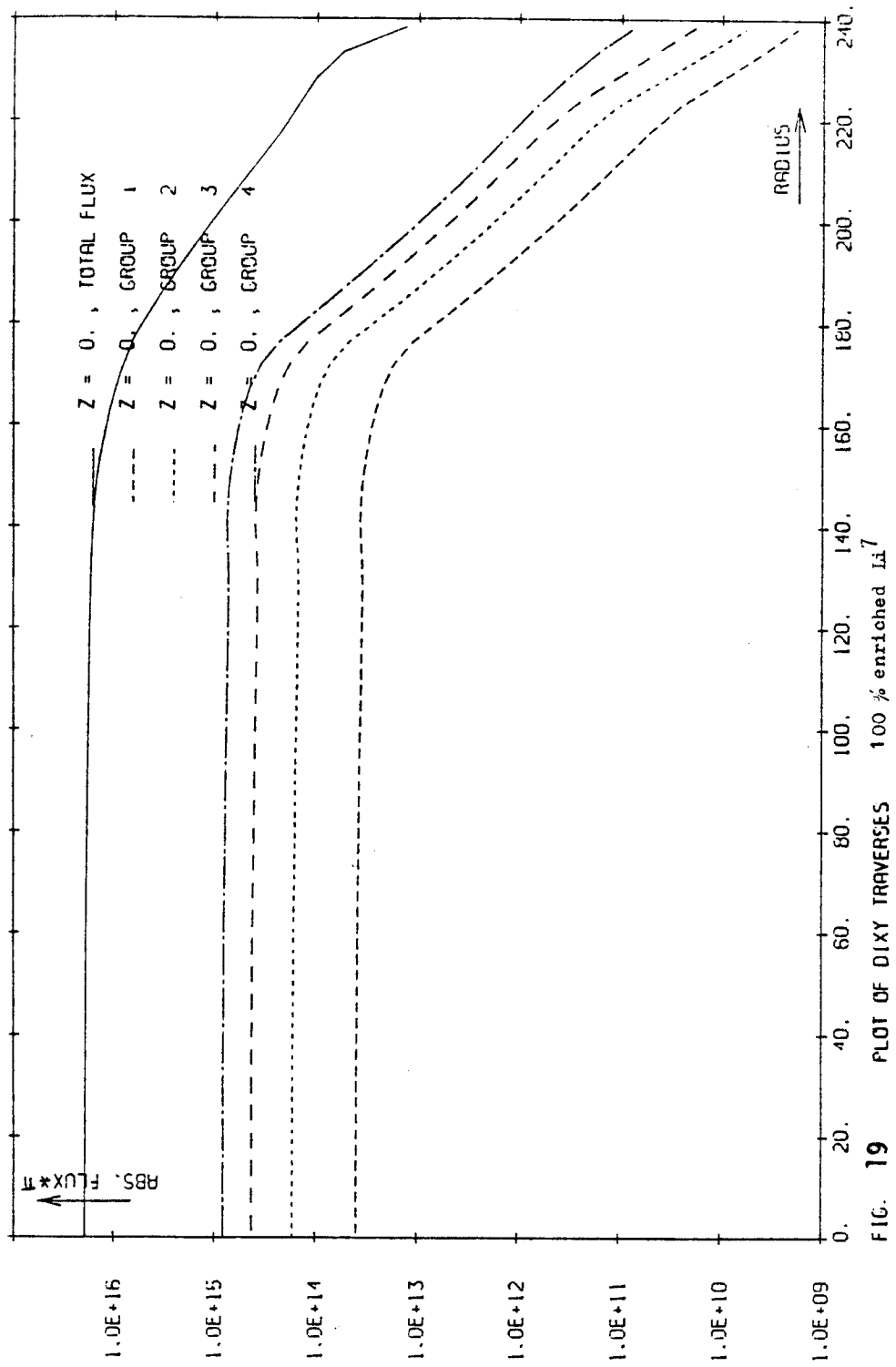


FIG. 19 PLOT OF DIXY TRAVERSES

and

- x Isotope identification
- y Reaction type identification
- i Energy group index

#### Tritium Production with 100% Enriched $\text{Li}^7$ Coolant

Table XV shows the results from DIXY for material  $\text{Li}^7$ , type  $\sigma_{(n,n',\text{total})}$  and the resulting tritium production with the help of the ratios of Table XIV. To obtain  $3000 \text{ MW}_{\text{th}}$  with an energy release of 193 MeV/fission, the normalized flux must be multiplied by  $F = 2.26 \times 10^{+19}$ . The tritium production from 100%  $\text{Li}^7$  is:

- With the ENDF/B-II data:

$$1.98 \times 10^{+18} \text{ tritium atoms/sec} = 9.87 \text{ g/sec} = 0.853 \text{ g/MWth day}$$

$$= \underline{249} \text{ g/GWe year}$$

- With the Wisconsin data

$$= \underline{345} \text{ g/GWe year}$$

#### Tritium Production from Natural Lithium

Table XVI shows the results from DIXY for material  $\text{Li}^6$ , type  $\sigma_{n,\alpha,T}$  and of material  $\text{Li}^7$ , type  $\sigma_{(n,n',\text{total})}$  with corresponding tritium production. In this case the multiplication factor for the flux is  $F = 2.27 \times 10^{19}$ . The tritium production from natural lithium is:

- With ENDF/B-III data

$$5.61 \times 10^{19} \text{ tritium atoms/sec} = 2.80 \times 10^{-4} \text{ g/sec} = 24.2 \text{ g/MWth}$$

$$= \underline{7.06} \text{ kg/GWe year}$$

- With Wisconsin data

$$= \underline{7.15} \text{ kg/GWe year}$$

Table XIV  
Inelastic Scattering Data for  $\text{Li}^7$

Group	$\langle \sigma_{n,n',\text{Total}} \rangle^{\text{K}}$	$\langle \sigma_{n,n'(\alpha,T)} \rangle^{\text{K}}$	$\langle \sigma_{n,n'(\alpha,T)} \rangle^{\text{W}}$	B/A	C/A
1	0.629	0.418	0.4158	0.665	0.661
2	0.452	0.172	0.2450	0.381	0.542
3	0.233	0.0045	0.01853	0.019	0.080
4	0.197	0	-	-	-
5	0.149	0	-	-	-
6	0.018	0	-	-	-
7	0	0	-	-	-

Table XV Tritium Production Per Source Neutron/Sec for 100%  $\text{Li}^7$ 

Group	$i_{R(n,n',\text{total})}^{\text{Li}^7}$	Tritium rate ENDF/B-III Data	Tritium rate Wisconsin Data
1	$3.667 \cdot 10^{-3}$	$2.439 \cdot 10^{-3}$	$2.424 \cdot 10^{-3}$
2	$11.213 \cdot 10^{-3}$	$4.272 \cdot 10^{-3}$	$6.077 \cdot 10^{-3}$
3	$14.684 \cdot 10^{-3}$	$0.280 \cdot 10^{-3}$	$1.175 \cdot 10^{-3}$
4	$24.181 \cdot 10^{-3}$	-	-
5	$25.104 \cdot 10^{-3}$	-	-
6	$5.859 \cdot 10^{-3}$	-	-
7	-	-	-
Total	$84.708 \cdot 10^{-3}$	$6.991 \cdot 10^{-3}$	$9.676 \cdot 10^{-3}$

Table XVI Tritium Production Per Source Neutron/Sec for Natural Lithium

Group	$i_{R\text{Li}^7}$ (n,n',total)	Tritium rate ENDF/B-III	Tritium rate Wisconsin	$R_{n,\alpha,T}^{\text{Li}^6}$
1	$3.345 \cdot 10^{-3}$	$2.224 \cdot 10^{-3}$	$2.211 \cdot 10^{-3}$	
2	$10.184 \cdot 10^{-3}$	$3.880 \cdot 10^{-3}$	$5.520 \cdot 10^{-3}$	
3	$13.259 \cdot 10^{-3}$	$0.252 \cdot 10^{-3}$	$1.061 \cdot 10^{-3}$	
Total Li <sup>7</sup>	$76.229 \cdot 10^{-3}$	$6.356 \cdot 10^{-3}$	$8.792 \cdot 10^{-3}$	
1-26				$190.509 \cdot 10^{-3}$
Total Li		$196.865 \cdot 10^{-3}$	$199.301 \cdot 10^{-3}$	

### Reactor Parameters for Lithium Cooled Systems

The higher fissile inventory needed with lithium cooling makes most of the reactor parameters worse. Table XVII shows some important system parameters.

For sodium, natural lithium and 100%  $\text{Li}^7$  coolants the first four columns show the changes in fuel inventory. We observe a slight increase of fissile material for 100%  $\text{Li}^7$  coolant and a significant increase for natural lithium compared to sodium. The  $k_{\text{eff}}$  values in the next columns are some percent above 1. The void effect, calculated from 4-group 2-dimensional diffusion calculations, increases by a factor of 3 for 100%  $\text{Li}^7$  and by a factor  $>10$  for natural lithium. The breeding ratio decreases for 100%  $\text{Li}^7$  and becomes smaller than 1 for natural lithium.

In order to obtain some qualitative information about the void effect and the Doppler effect with lithium cooling, some  $k_{\infty}$  calculations were performed. The benchmark investigations have shown that the influences of system changes on void effect and Doppler effect may be predicted qualitatively from these  $k_{\infty}$  calculations.

Table XVIII shows the results of the  $k_{\infty}$  calculations for the inner core mixture. The results of Table XVII for the void effect are qualitatively rather well confirmed by the results of Table XVIII.

The Doppler effect has been calculated for a temperature change 500 K  $\rightarrow$  1000 K for the heavy isotopes. In the 100%  $\text{Li}^7$  case the normal Doppler effect increases about 15% (caused by spectrum softening) and decreases about 5% for the voided reactor (due to the changes of isotope number densities and spectral shift). For the natural lithium case the Doppler effect is decreased significantly (~factor 2).



Table XVII  
System Parameters LMFBF's

Coolant	Inner core mixture				$k_{\text{eff}}$ Reactor *)		$\frac{\Delta k_v}{k}$	B.R. (C.R.)
	U'/U	Pu'/Pu	Pu/U	Fiss/Fert	normal	void		
Na	1.	1.	0.148	0.115	1.02400	1.04271	$1.83 \cdot 10^{-2}$	1.356
100 % Li <sup>7</sup>	0.997	1.05	0.157	0.121	1.02453 1.02674*)	1.08323*)	$5.4 \cdot 10^{-2}*)$	1.282
Nat Li	0.95	1.4	0.218	0.166	1.03115 1.03421*)	1.27197*)	$23.0 \cdot 10^{-2}*)$	0.922

\*) 4-group calculations, otherwise 26 groups

Table XVIII  
 $k_{\infty}$  Calculations for Inner Core Mixture

Coolant	void effect		Doppler effect *)	
	Normal	Hot	Normal	Void
Na	1.	1.	1.	1.
100 % Li <sup>7</sup>	2.0	1.9	1.14	0.95
Nat. Li	6.2	5.9	0.42	0.65

\*) Temperature change 500 → 1000 K for heavy isotopes

### Improvement of the Fission Reactor Models

The previous investigations showed that the replacement of sodium by lithium in a LMFBR with U-Pu fuel is not favorable for the production of tritium in a fission reactor.

In the case of 100%  $\text{Li}^7$  coolant the void effect is rather large (two times the void effect with sodium cooling) and the tritium production is too small ( $\sim 0.3$  kg T/GWe year).

Cooling with natural lithium (7.42%  $\text{Li}^6$ ) leads to very bad conversion ratios, very high void effects and good tritium production from the (n- $\alpha$ )-reaction of  $\text{Li}^6$  ( $\sim 7$  kg T/GWe year).

These results lead to the following proposals for possible tritium producers:

- a. Moving the  $\text{Li}^6$  absorber from the core into the radial blanket for tritium production. This could be done both with sodium and lithium cooling.
- b. Avoiding large void effects by the use of Th- $\text{U}^{233}$  fuel instead of U-Pu fuel. The Th- $\text{U}^{233}$  fuel has a smaller breeding ratio but better void effect.

### Sodium Cooled LMFBR with U-Pu Fuel with Lithium Radial Blanket

In the benchmark reactor the radial blanket has been replaced by a natural lithium blanket with about 20% structural material and 80% lithium. The applied atom number densities are given in Table XIX.

Table XIX  
Atom Number Densities in atoms/barn-cm  
of Radial Blanket

Fe	8.9587E-3
Ni	1.7397E-3
Cr	2.5464E-3
Mo	0.1814E-3
Li-6	1.8194E-3
Li-7	23.6100E-3

The value of  $K_{\text{eff}}$  decreased by less than 1%

The tritium production in the blanket caused by the  $\text{Li}^6$  (n- $\alpha$ )-processes gives a reaction rate integral from the 2-dimensional 4 group DIXY-calculation:

$$R_{n,\alpha,T}^{\text{Li}^6} = 0.0383$$

being equivalent to about 1.3 kg T/GW<sub>e</sub> year. The breeding ratio of this system is BR = 1.21 (about -0.15 compared to the reference system).

Further parametric calculations with different  $\text{Li}^6$  fractions and different blanket thickness resulted in values for the rate integral  $R(\text{Li}^6, n, \alpha, T)$  between 0.037 and 0.055. This means a tritium production between 1-2 kg T/GWe year. The neutronic behavior of this system is satisfactory.

#### Lithium Cooled LMFBR with Th-U<sup>233</sup> Fuel and Lithium Radial Blanket

The 26-group constants for Th-232, U-233,  $\text{Li}^6$  and  $\text{Li}^7$  are recalculated from ENDF/B IV data using a weighting spectrum of a sodium cooled LMFBR.

For the fuel the following data was used:

- density  $\text{UO}_2$   $10.5 \text{ g/cm}^3$
- $\text{ThO}_2$   $9.69 \text{ g/cm}^3$
- fuel fraction 41%
- smear density of fuel 91%

From these data a fuel atom number density,  $\text{NF} = 8.2441\text{E-}3 \text{ atoms/barn-cm}$ , has been calculated.

Two cases have been calculated:

- 100%  $\text{Li}^7$  coolant
- 1%  $\text{Li}^6$ , 99%  $\text{Li}^7$  coolant

The reactor geometry, the blankets and the reflector were the same as in the sodium cooled LMFBR with U-Pu.

Th- $\text{U}^{233}$  System with 100%  $\text{Li}^7$  Coolant

The following data were computed:

	Th/U233	$k_\infty$
Core 1	8.	1.15275
Core 2	6.	1.31787

$$K_{\text{eff}} = 1.00413$$

$$R_{\text{n}, \alpha, T}^{\text{Li-6}} = 0.0364 \quad \# \quad \sim 1 \text{ kg T/GW}_e \cdot \text{year}$$

$$R_{\text{n}, \text{n}'}^{\text{Li-7}} = 0.0931 \quad \# \quad \sim 0.4\text{-}0.5 \text{ kg T/GW}_e \cdot \text{year}$$

The system has a breeding ratio of  $BR = 1.02$ . Voiding of the driver zones and the axial blanket gives  $K_{eff} = 0.991569$ . That means a negative void coefficient of  $DKV = 1.25E-2$ .

Th-U<sup>233</sup> System with 1% Li<sup>6</sup> Fraction Coolant

The following data were computed:

	Th/U233	$k_{\infty}$
Core 1	7.5	1.15418
Core 2	5.6	1.32059

$$K_{eff} = 1.00955$$

Blanket :

$$R_{n,\alpha,T}^{Li-6} = 0.0353$$

$$R_{n,n'}^{Li-7} = 0.0059$$

Coolant :

$$R_{n,\alpha,T}^{Li-6} = 0.0344$$

$$R_{n,n'}^{Li-7} = 0.0857$$

These figures show that the coolant produces about the same amount of tritium as the blanket. The system has a conversion ratio of  $CR = 0.95$ . Voiding of the driver zones and the axial blanket gives  $K_{eff} = 1.02845$ . Void effect  $DKV = 1.89E-2$ , comparable with the Na/U-Pu system.

These calculations show that tritium breeding is possible in the radial blanket of conventional LMFBR reactors. The breeding ratio of Na/U-Pu reactors will remain  $>1.1$ . The application of Li/Th- $U^{233}$  systems can increase the tritium production by adding  $Li^6$  to the coolant. The conversion ratio for these systems varies between 0.95 and  $>1$ .

Two new features are now introduced.

- Use of  $Li_2O$  instead of liquid lithium.
- Extending the tritium breeding to the axial blanket too.

Both features lead to increased tritium production without worsening the neutronic behavior. However, tritium breeding in the blanket decreases the breeding ratio significantly.

The following calculations were performed with the methods described earlier.

#### LMFBR with $Li_2O$ Radial Blanket

In the reference benchmark reactor with sodium cooling and U/Pu fuel, the radial blanket has been replaced by a  $Li_2O$  blanket with the following properties:

- $Li_2O$  fraction 80%
- Can fraction 20%
- Smear density  $Li_2O$  90%
- Atom density  $Li_2O$   $8.2E-2$  atoms/barn-cm
- $Li^6$  enrichment 90%

In order to maintain criticality and a rather flat power distribution, the fuel enrichment of the driver zones had to be modified in the following way.

- Inner core

+ U multiplied by 1.001

+ Pu multiplied by 0.99

The resulting  $k_{\infty}$  amounts to  $k_{\infty} = 1.343967$ .

Calculations with DIXCON/DIXY gave the following results:

Table XX

DIXCON/DIXY Results (Accuracy 1%)

<u>Groups</u>	<u>4</u>	<u>11</u>	<u>26</u>
$K_{\text{eff}}$ reference reactor	1.022302	1.010480	1.019946
$K_{\text{eff}}$ voided reactor	1.040477	1.036003	1.0363340
$K_{\text{eff}}$ hot reactor*	1.015363	1.012748	1.013108
Void effect DKV	1.82E-2	1.65E-2	1.64E-2
Doppler effect DKT*	-0.69E-2	-0.67E-2	-0.68E-2

---

\*Hot reactor means fuel temperature increases from 1100 K to 2200 K.

The values of DKV and DKT are comparable with the results for the original benchmark reactor.

The reactor reaction rate integral for  $\text{Li}^6$  capture per sec per fission source neutron is:

$$R_{\text{C}}^{\text{Li}^6} = 4\pi * 0.0592 = 0.744 \text{ T-atoms/sec fiss. neutr.}$$

The flux factor to generate 1 GWth is:

$$F = 7.54E + 18$$

For 100% load factor the conversion factor FM between (T-atoms/sec fiss. neutr.) and (kg T/GWth year) is given by:

$$FM = F \cdot 3600 \cdot 24 \cdot 365.25 \cdot 1.E-3 \cdot 3 / 6.02E+23 = 1.57E-19 \cdot F$$

Also in the case the T-production at the beginning of life amounts to:

$$0.744 \cdot 1.573E-19 \cdot 7.54E+18 = \underline{0.882} \text{ kg T/GWth year}$$

The breeding ratio of the system is

$$BR = 1.11 \text{ (-0.25 compared to the original benchmark model)}.$$

Thus, this model shows satisfactory neutronic behavior but a somewhat low T-production. From other calculations it doesn't seem possible to increase the T-production in the radial blanket of this reactor type significantly.

#### LMFBR with Li<sub>2</sub>O Radial and Axial Blanket

In the next step the fuel of the axial blanket has been replaced by Li<sub>2</sub>O as specified for the radial blanket. The sodium coolant has been kept.

The fuel composition of the inner core has not been changed with respect to the original benchmark reactor.

In the outer core the Pu-content has been multiplied by a factor of 1.08, the U-content by 0.996. The value of  $k_{\infty} = 1.355776$ .

The results from the DIXCON/DIXY calculations are

- $K_{eff}$ 
  - 4 groups 1.009096
  - 11 groups 1.007401
- Reaction integrals for Li<sup>7</sup> capture (T-production) :
  - + radial blanket 0.0651\*4 $\pi$  T-atoms/sec fiss. neutr.
  - + axial blanket 0.0718\*4 $\pi$  T-atoms/sec fiss. neutr.
- Flux factor for 1 GWth
  - $F = 7.55E + 18$



- T-production per GWth Year

$$+ \text{ radial blanket } 1.573\text{E-}19 \cdot F \cdot 0.0651 \cdot 4 \cdot \pi = 0.972 \text{ kg}$$

$$+ \text{ axial blanket } 1.573\text{E-}19 \cdot F \cdot 0.0178 \cdot 4 \cdot \pi = 1.072 \text{ kg}$$

$$\text{Total} = \underline{\underline{2.044}} \text{ kg}$$

- Due to the replacement of the axial blanket by  $\text{Li}_2\text{O}$ , the breeding ratio has decreased significantly. This system has a conversion ratio  $\text{CR} = 0.94$ .

We can observe that the replacement of the axial blanket by  $\text{Li}_2\text{O}$  about doubles the total T-production. The neutronic behavior also is satisfactory. Only the breeding ratio has decreased significantly.

#### LMFBR with $\text{Li}_2\text{O}$ Radial and Mixed ( $\text{Li}_2\text{O}$ -U) Axial Blanket

The large decrease in the breeding ratio in the case where the axial blanket is replaced by  $\text{Li}_2\text{O}$  can be avoided if only a part of the axial blanket is replaced by  $\text{Li}_2\text{O}$ . Fig. 20 shows a possible configuration.

The fuel composition of the inner core has not been changed with respect to the original benchmark reactor.

In the outer core the Pu content has been multiplied by a factor of 1.07 and the U content by 0.996. The value of  $k_\infty = 1.353783$ .

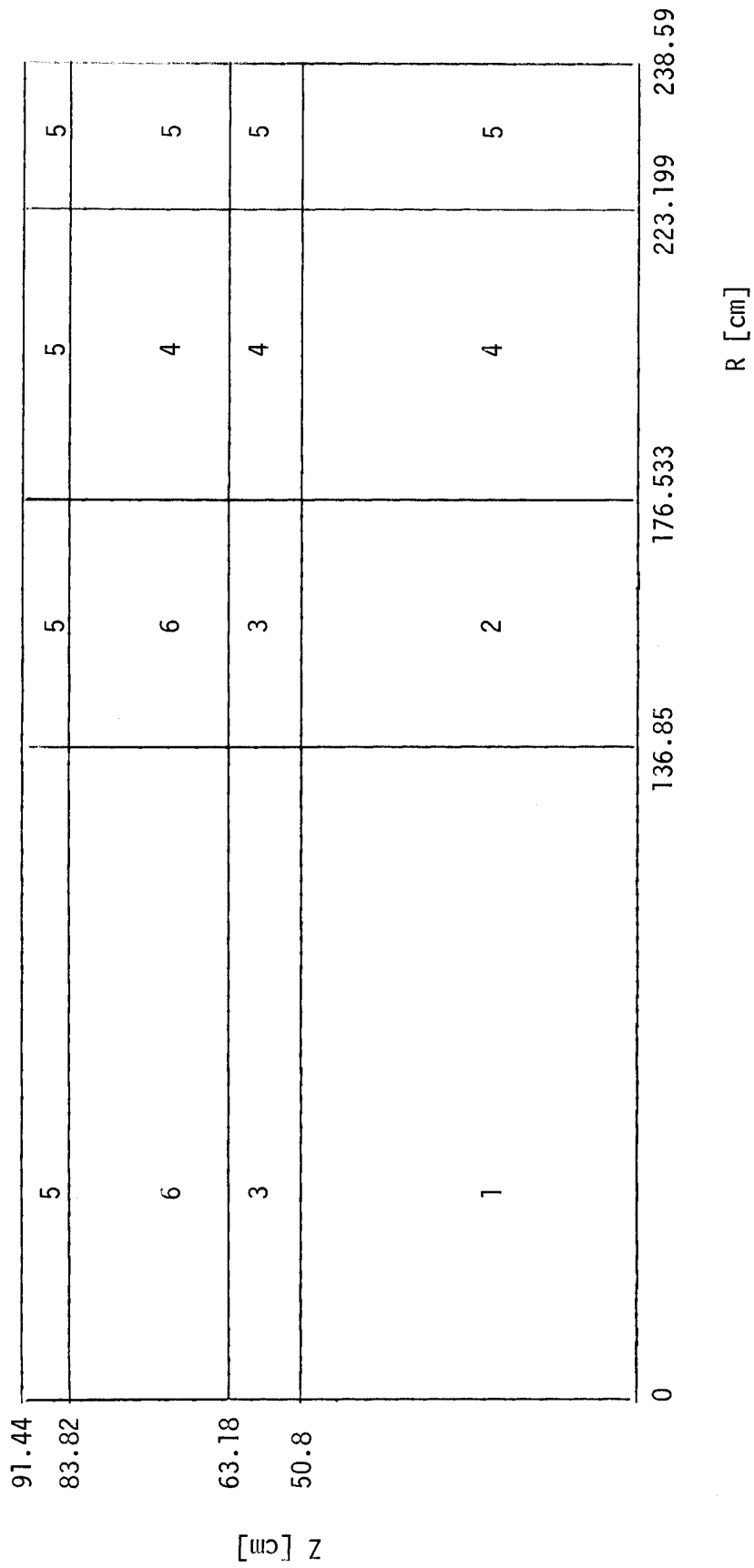
The results from the DIXCON/DIXY calculations are

-  $K_{\text{eff}}$

4 groups	1.020288
11 groups	1.017905
26 groups	1.018214

- Reaction integrals for  $\text{Li}^6$  capture (T-production):

+ radial blanket	$0.0613 \cdot 4 \cdot \pi$	T-atoms/sec fiss. neutr.
+ radial blanket	$0.0328 \cdot 4 \cdot \pi$	T-atoms/sec fiss. neutr.



Mixture

- 1 inner core
- 2 outer core
- 3 axial blanket (benchmark specification)
- 4 radial  $\text{LiO}_2$  blanket (80%  $\text{LiO}_2$ )
- 5 reflector
- 6 axial  $\text{LiO}_2$  blanket (40%  $\text{LiO}_2$ )

FIGURE 20  
(R-Z Model)

- Flux factor for 1 GWth

$$F = 7.58E + 18$$

- T-production per GWth year

$$+ \text{ radial blanket } 1.573E-19 * F * 0.0613 * 4 * \pi = 0.918 \text{ kg}$$

$$+ \text{ axial blanket } 1.573E-19 * F * 0.0328 * 4 * \pi = 0.491 \text{ kg}$$

$$\text{Total} = \underline{\underline{1.397}} \text{ kg}$$

- This system has a breeding ratio slightly larger than one

$$\text{BR} - 1.06.$$

### Conclusions

The results of these calculations are summarized in Table XXI. Cases 1 and 2 are actually unacceptable because the coolant void coefficient of reactivity is very large and positive. For the other cases the void coefficient is okay. Case 6 is quite interesting because of the high production rate. However the fissile conversion ratio falls below one for this configuration (CR = 0.94). In case 7, some fissile and fertile fuel is added to the axial blanket to bring the fissile breeding ratio back to one. This comes with a very severe penalty to the tritium breeding which has fallen by 30% from Case 6.

Table XXI  
Summary of LMFBR Calculations

<u>Case</u>	<u>T-Production kg/MW<sub>t</sub>-year</u>
1) LMFBR with Na coolant replaced by 100% <sup>7</sup> Li	1.05 x 10 <sup>-4</sup>
2) LMFBR with Na coolant replaced by nat. Li	2.96 x 10 <sup>-3</sup>
3) LMFBR with Na coolant, radial blanket replaced by 80% Li and 20% structure	5.46 x 10 <sup>-4</sup>
4) LMFBR with Li coolant, Th- <sup>233</sup> U fuel and Li radial blanket	
100% <sup>7</sup> Li coolant	6.3 x 10 <sup>-4</sup>
1% <sup>6</sup> Li-99% <sup>7</sup> Li coolant	----
5) LMFBR with Na coolant, Li <sub>2</sub> O in the radial blanket 90% enriched in <sup>6</sup> Li	8.82 x 10 <sup>-4</sup>
6) LMFBR with Na coolant, Li <sub>2</sub> O in the radial and axial blanket	2.04 x 10 <sup>-3</sup>
7) LMFBR with Na coolant, Li <sub>2</sub> O radial blanket and mixed Li <sub>2</sub> O and U-Pu axial blanket	1.4 x 10 <sup>-3</sup>

## V. Heavy Water Reactors

Tritium is produced in the moderator and coolant of heavy water reactors by neutron capture in deuterium. This produces  $1.9 \times 10^{-4}$  kg/MW<sub>e</sub>-yr.

## VI. Fuel Reprocessing Plants

Tritium is generated in LWRs by ternary fission. An amount of 500-1000 Ci/1000 MW(e)-yr is generated by neutron capture reactions, primarily in the shim control boron in the primary coolant.

Tritium generation by the year 2000 would amount to a meager 51.3 g/yr for a 683.9 GWe installed capacity, or 32.6 g/yr for a 434 GWe installed capacity. This amounts to only  $1.18 \times 10^{-6}$  kg/MW<sub>e</sub>-yr of tritium production.

## VII. Dedicated Fusion Reactors

Generation of tritium from dedicated fusion reactors is the exact equivalent of reserving a portion of the solid angle in the hybrid to only tritium breeding. Hence, this option can be viewed as simply a hybrid reactor with a fissile production blanket and a tritium production blanket. The exact details of the blanket design will depend strongly on the type of fusion device. There appears, therefore, to be little evidence that a dedicated tritium producing fusion reactor will be an attractive combination with a hybrid. Furthermore, since the goal of removing the tritium function from the hybrid is to speed the introduction, it is unlikely that a dedicated fusion reactor is the answer.

### VIII. Conclusions

A summary of the tritium capabilities of the various sources discussed in this report are given in Table XXII. Clearly the dedicated Savannah River type fission reactors produce the greatest amount of tritium, but they also produce no power. It is possible to produce significant amounts of tritium in greatly modified LWRs but this of course would require a long list of institutional changes before implementation is allowed. The final conclusions must come from economic considerations about the price of coupling the hybrid to an external tritium producing system. This compilation of tritium sources and their potential production capabilities should provide input to these final conclusions.

Table XXII Possible Tritium Producing Sources

Source	Production kg/(MWe·year)	Remarks
Existing Light Water Reactors (LWRs)	$7.50 \times 10^{-8}$	From shim control boron
Heavy Water Reactors	$1.90 \times 10^{-4}$	Activation of D <sub>2</sub> O
Fuel Reprocessing	$1.18 \times 10^{-6}$	Ternary fission tritium
Liquid Metal Fast Breeder	$5.1 \times 10^{-3}$	Li <sub>2</sub> O used in the axial and radial blankets
Savannah River Reactors	$\sim 1.66 \times 10^{-2}$	Maximum, No power production
Hanford N-Reactor	$4.34 \times 10^{-3}$	Minimum + Pu + power
	$1.14 \times 10^{-2}$	Maximum, No Pu, + power

Fuel Consumption in Fusion Reactors: 0.11 - 0.17 kg/(MWe·year)

References

1. T. Rhinehammer, L. Wittenberg, "An Evaluation of Fuel Resources and Requirements for the Magnetic Fusion Energy Program", MLM-2418, Mound Laboratory (Oct. 1978).
2. Information obtained from Savannah River Laboratory. Also, "The Savannah River High Flux Demonstration", DP-999, E.I. du Pont de Nemours and Co. (June 1965).
3. G. Kessler, Karlsruhe Nuclear Research Center, Karlsruhe, W. Germany, private communication.
4. "Specifications for an International Comparison Calculation of a Large Sodium Cooled Fast Breeder Reactor," to be published by ANL in Proc. of the Specialists Meeting, 7-9 Feb., 1978.